Effect of high-energy mechanical milling on the medium-range ordering in glassy As-Se

Yaroslav Shpotyuk, Pavlo Demchenko, Zdenka Bujnakova, Peter Balaz, Catherine Boussard-Plédel, Bruno Bureau, Oleh Shpotyuk

▶ **To cite this version:**

Yaroslav Shpotyuk, Pavlo Demchenko, Zdenka Bujnakova, Peter Balaz, Catherine Boussard-Plédel, et al.. Effect of high-energy mechanical milling on the medium-range ordering in glassy As-Se. Journal of the American Ceramic Society, 2020, 103 (3), pp.1631-1646. 10.1111/jace.16877 . hal-02470150

HAL Id: hal-02470150
https://univ-rennes.hal.science/hal-02470150

Submitted on 30 Aug 2024

HAL is a multi-disciplinary open access archive for the deposit and dissemination of scientific research documents, whether they are published or not. The documents may come from teaching and research institutions in France or abroad, or from public or private research centers.

L'archive ouverte pluridisciplinaire **HAL**, est destinée au dépôt et à la diffusion de documents scientifiques de niveau recherche, publiés ou non, émanant des établissements d'enseignement et de recherche français ou étrangers, des laboratoires publics ou privés.

Effect of high-energy mechanical milling on the medium-range ordering in glassy As-Se

Yaroslav Shpotyuk [1,2,*], Pavlo Demchenko [2], Zdenka Bujňáková [3], Peter Baláž [3], Catherine Boussard-Pledel [4], Bruno Bureau [4], Oleh Shpotyuk [5,6]

[1] Institute of Physics, University of Rzeszow, Rzeszow, Poland
[2] Ivan Franko National University of Lviv, Lviv, Ukraine
[3] Institute of Geotechnics of SAS, Košice, Slovakia
[4] Univ Rennes, CNRS, ISCR [(Institut des Sciences Chimiques de Rennes)] – UMR 6226, Rennes, France
[5] Jan Dlugosz University in Czestochowa, Czestochowa, Poland
[6] O.G. Vlokh Institute of Physical Optics, Lviv, Ukraine

* Email: yashpotyuk@gmail.com

Abstract

Effect of high-energy mechanical milling on glassy As_xSe_{100-x} ($5 \le x \le 75$) is recognized with X-ray powder diffraction analysis applied to their diffuse halos ascribed to intermediate—and extended-range structural ordering, which are revealed respectively in the first sharp diffraction peak (FSDP) and principal diffraction peak (PDP). Straightforward interpretation of the results is developed within *modified microcrystalline approach*, treating diffuse halos as superposition of broadened Bragg-diffraction reflexes from remnants of *inter-planar correlations*, supplemented by *inter-atomic* Ehrenfest-diffraction reflexes from most prominent *inter-atomic* and *inter-molecular correlations* between cage-like molecules (such As_4Se_4 and/or As_4Se_3). Milling is shown to be ineffective in glassy arsenoselenides near Se ($x < 20$), while causing increase in the FSDP width for glasses with $20 \le x \le 40$ due to destroyed inter-planar ordering. Remnants of cage-like molecules in over-stoichiometric As-rich As_xSe_{100-x} glasses ($40 \le x \le 75$) disappear under milling, promoting formation of higher polymerized structural network. This milling-driven *reamorphization* results in a drastic increase in the FSDP position and *fragmentation* impact on the correlation length of the FSDP-responsible entities. Breakdown in intermediate-range ordering in these glasses is accompanied by changes in their extended-range ordering revealed in high-angular shift and broadening of the PDP. This effect is concomitant with the disappearance of distant inter-atomic correlations between quasi-crystalline planes in the milled arsenoselenide glasses at a cost of prolonged correlations dominating in their extended-range ordering.

1. INTRODUCTION

Nowadays, nanostructurized substances attract unprecedented attention in the materials science community due to a great variety of unexpected and practically important applications.[1] That is why high-energy mechanical milling (MM) as an advanced nanostructurization tool transferring condensed matter to nanoscopic length-scale has been widely applied to crystalline solids, allowing the generation of defects tending them towards out-of-equilibrium high-entropy state.[2, 3] However, because of native metastability proper to disordered state, the consequences of MM are merely hidden for glasses derived by conventional melt-quenching. Being nanostructurized, they reveal deeply depressed glass-transition temperatures T_g and respectively accelerated ability to

physical aging,[4-8] while an adequate picture of responsible nanostructure transformations remains rather unclear.

In this work, we first report the results of high-energy MM effect on medium-range structural ordering in glassy arsenoselenides As_xSe_{100-x} obtained from the glass-forming region of this canonical system,[9, 10] including preliminary studied *under-stoichiometric* glasses restricted by *stoichiometric* As_2Se_3 (ie $As_{40}Se_{60}$) and Se-rich As_5Se_{95} specimens,[11] and stretching far towards *over-stoichiometric* glassy $As_{65}Se_{35}$ and mixed crystalline-amorphous $As_{70}Se_{30}$ and $As_{75}Se_{25}$ alloys.

2. EXPERIMENTAL DETAILS

Arsenoselenide As_xSe_{100-x} alloys of under-stoichiometric Se-rich (x = 5, 10, 15, 17.5, 20, 22.5, 25, 29, 33, 35, 37) and over-stoichiometric As-rich compositions (x = 45, 50, 55, 60, 65, 70, 75) in respect to stoichiometric As_2Se_3 (x = 40, ie $As_{40}Se_{60}$) were synthesized by rapid melt-quenching inwater from high-purity elemental precursors (As and Se of 5N purity) as described in details given elsewhere.[11, 12] The synthesized As_xSe_{100-x} alloys with $5 \le x \le 65$ were completely amorphous, as it follows from their X-ray powder diffraction (XRPD) patterns showing only diffuse "amorphous" peak-halos proper to glassy state, conch-like fracture of fresh-ingot cut sections and IR transparency of polished cut-plates. The $As_{70}Se_{30}$ and $As_{75}Se_{25}$ alloys (close to the border of glass-forming region in As-Se system)[9, 10] were partially crystalline, their XRPD profiles being rich on sharp reflexes ascribed to As phase.

The plane-parallel disks of 1.0-1.5 mm thickness cut from bulky ingots (1 hour annealed at the temperature T_a of 15-20°C below glass-transition temperature T_g) were used as reference samples. The macroscopic densities ρ (± 0.005 g·cm^{-3}) determined at room temperature by Archimedes displacement in ethanol using Mettler Toledo balances, and mid-onset glass-transition temperatures T_g ($\pm$3°C) determined from differential scanning calorimetry under 10 K/min heating rate using TA Instrument Q20 calorimeter, testify on the adequacy of these alloys with known counterparts from As-Se system.[9-13]

The high-energy MM was performed in dry mode using Pulverissete 6 mill operated at protective argon atmosphere and 500 min^{-1} rotational speed for 60 minutes in 250 mL tungsten carbide chamber (loaded with 50 tungsten carbide balls each having 10 mm in diameter). Around 3 g of coarse-grained powder of each composition preliminary sieved under 200 μm was used for the MM. The amorphous state of these substances is not changed under MM, as it follows from stretched diffuse halos observed in their XRPD patterns.

The identity of the MM-derived phases in As_xSe_{100-x} was clarified by XRPD analysis of their diffuse halos applied, in part, to the *first sharp diffraction peak* (FSDP), which is believed to be signature of specific structural entities in vitreous substances forming a so-called *intermediate-range ordering* over a length scale of few tens of Å.[14]

The XRPD patterns were detected in *transmission mode* using a STOE STADI P diffractometer with a linear position-sensitive detector (Cu $K\alpha_1$-radiation, and a curved Ge monochromator on primary beam).[15] This experimental setup has an advantage in comparison with reflection geometry due to the possibility to remove undesirable low-angle reflections from sample holders and keep utmost reproducibility between multiple measuring cycles. The $2\Theta/\omega$-scanning was performed with

0.015 °2Θ step, the detector increment being 0.480 °2Θ within a whole range of scattering angles, while time of scanning being 500 seconds per step. The temperature was maintained during measurements at (25.0 ± 0.3)°C. XRPD patterns were corrected for empty instrument background, X-ray polarization, sample absorption, multiple and Compton scattering, Laue diffuse scattering and weighting correction, to obtain *total scattering structure function, S*(*Q*), and its expression as *reduced structure function*, $F(Q) = Q\,[S(Q)-1]$, where Q is the magnitude of the scattering wave vector.[16] The reduced X-ray structure factors, $F(Q)$, were calculated using the known PDFgetX2 program.[17] Preliminary data processing was performed using information on the structure of crystalline arsenoselenide polymorphs taken from databases,[18, 19] in part, the JCPDS cards No. 65-2365 for monoclinic As_2Se_3, No. 73-0465 for trigonal Se, No. 71-0388 for monoclinic As_4Se_4, No. 04-4979 for orthorhombic As_4Se_3, and No. 72-1048 for trigonal As. To visualize crystallographic details of some arsenoselenide phases, the programs DIAMOND and VESTA were employed.[20, 21]

Processing of the XRPD profiles was performed with STOE WinXPOW 3.03 and PowderCell 2.4 program packages, following normalization procedure with respect to the intensity of the maximum peak.[22, 23] Both peak angular position (2θ) and full width at half maximum (FWHM) were defined with ±0.05 °2θ accuracy, the values of *scattering vector Q* and *width* ΔQ in a reciprocal space were calculated as:

$$Q = (4\pi/\lambda) \times sin\ \theta, \quad (1)$$

$$\Delta Q = (4\pi/\lambda) \times sin\ (FWHM/2). \quad (2)$$

The *characteristic distance R* (spacing of the FSDP-responsible quasi-periodicity) and *correlation length L* (over which this quasi-periodicity was maintained) were defined as:[14, 24-31]

$$R = 2\pi/Q, \quad (3)$$

$$L = 2\pi/\Delta Q. \quad (4)$$

We also explore the concept of diffuse halos in the XRPD patterns of amorphous substances as arising from coordination spheres, ie the closest inter-atomic distances like in randomly packed multiparticulate systems,[32-35] when XRPD patterns are governed by the Ehrenfest relation[36]:

$$2d_s \cdot sin\ \theta = 1.23 \cdot \lambda, \quad (5)$$

where d_S is *average inter-atomic distance* in a glass structure (ie distance between atomic scattering centers defined as radius of the corresponding coordination sphere).

The accuracy in *R*, *L* and d_S determination doesn't exceed ±0.1 Å.

3 RESULTS AND DISCUSSION

3.1 Compositional variations in the XRPD patterns of glassy arsenoselenides

The XRPD patterns of unmilled and milled As_xSe_{100-x} alloys demonstrate few diffuse peaks ("amorphous" halos proper to vitreous arsenic chalcogenides)[24-31] at ~15-22, ~28-33 and ~50-60 °2Θ. In a reciprocal space, these halos can be scaled in respect to $Q \cdot d_S$ parameter (where d_S denotes an averaged nearest-neighbor inter-atomic distance), positioned at ~2-3, ~4.6-4.9, and ~7.7-8.9.[25-28] According to Fourier-transform analysis,[28, 29] each of these features corresponds to real-space ordering with effective *periodicity R* and *correlation length L* determined by Equations (3) and (4),

respectively. For inter-atomic distances of $d_s \cong$ 2.2-2.6 Å typical for arsenic chalcogenides (eg, $d_s \cong$ 2.43 Å corresponding to As-Se bond length in As_2Se_3),[9, 10] the first of these peaks associated with scales commensurable with *intermediate-range ordering* of some structural motifs, is reproduced in the structure factor $S(Q)$ as the FSDP positioned at $Q_1 \cong$ ~1-1.5 $Å^{-1}$. Noteworthy, under the same inter-atomic distances d_s, the second peak at ~28-33 $^o2\Theta$ (also quite sharp in a width) ascribed to sizes of these network-forming motifs, which are deterministic for so-called *extended-range ordering* in a glass[14] is revealed near scattering vectors Q_2 approaching ~1.8-2.2 $Å^{-1}$. For glassy networks composed of directional covalent-bonded units, this peak is referred to as the principal diffraction peak (PDP), ie the PDP in terms of,[28] or, alternatively, the SSDP, ie the second sharp diffraction peak in the Elliott's terminology.[37] The third diffuse peak (TDP)-halo, widely stretched at ~50-60 $^o2\Theta$ (corresponding to Q_3 ~3.3-4.0 $Å^{-1}$) is associated with shortest nearest-neighbor separations in a glass.[28] Within further consideration, it will be referred to as the TDP.

The experimental XRPD profiles in the angular diffraction 2Θ-range corresponding to the FSDP and PDP for some unmilled As-Se samples (under-stoichiometric glassy As_5Se_{95}, stoichiometric $As_{40}Se_{60}$, and over-stoichiometric $As_{50}Se_{50}$) as compared with calculated ones are shown in Figure 1. The XRPD patterns of unmilled and dry-milled As_xSe_{100-x} demonstrate three diffuse halos for glassy under-stoichiometric ($5 \le x \le 40$) and over-stoichiometric ($40 \le x \le 65$) specimens that are depicted in Figures 2 and 3, respectively. Similar compositional tendencies are also revealed in the low-Q part of the reduced X-ray structure factor $F(Q) = Q(S(Q)-1)$ for these glasses depicted in Figure 4. These changes in As_xSe_{100-x} are summarized for the FSDP (Figures 5-7) and PDP (Figure 8) accepting each peak-halo as a single diffuse component in the experimental XRPD pattern.

Thus, it is clearly seen that with increase in Se content in under-stoichiometric As_xSe_{100-x} (decrease in x parameter), the FSDP position shifts to higher scattering vectors Q_1 (Figures 2, 4, 5A), this effect for unmilled glasses being in an excellent agreement with known data.[30, 31, 38] The FSDP becomes merely reduced in a height and broadened in a width ΔQ_1 reaching a maximum near eutectic $As_{20}Se_{80}$ composition, and then rapidly drops with Se content (Figures 2, 4, 5B), these changes agreed with our preliminary research.11 Contrary to the FSDP, the PDP reveals an opposite steady tendency with x decrease in peak position Q_2 (decrease, Figure 8A) and width ΔQ_2 (increase, Figure 8B). So approaching glassy Se in under-stoichiometric As_xSe_{100-x}, the intermediate-range order due to the FSDP disappears, being covered by extended-range order due to low-Q shifted PDP at ~26-28 $^o2\Theta$ (Figure 1A) corresponding to Q_2 ~1.6-1.7 $Å^{-1}$ (see Figure 4). In the structure factor $F(Q) = Q(S(Q)-1)$ determination for unmilled As_2Se_3, the FSDP parameters reach $Q_1 = 1.28$ $Å^{-1}$ and $\Delta Q_1 = 0.43$ $Å^{-1}$ (see Figure 4, curve 12), while the PDP at $Q_2 = 2.23 Å^{-1}$ is more broadened having 0.54 $Å^{-1}$ in a width ΔQ_2.

With going from glassy As_2Se_3 to As-rich side (increase in x parameter), the FSDP gets increased in a height, becoming evidently sharper owing to strong narrowing in a width ΔQ_1 (Figure 5B), thus resulting in more prolonged correlation lengths L (Figure 6B). Under this trend, the FSDP position shifts towards lower Q_1 (Figure 6A) resulting in enlarged R (Figure 6A), these changes being close to saturation at high As content. Similarly, the PDP demonstrates the same decreasing tendencies in both peak position Q_2 and width ΔQ_2 with As content, resulting in saturation at 60-70 at. % As (see

Figure 8). Therefore, the FSDP and PDP are still well distinguishable in $As_{65}Se_{35}$ as it is illustrated by curve 17 in Figure 4. Other As-rich alloys ($As_{70}Se_{30}$, $As_{75}Se_{25}$) are amorphous-crystalline, their parameterization being performed after subtracting sharp reflexes from competitive crystalline phases.

3.2 Milling-driven changes in the XRPD patterns of glassy arsenoselenides

The FSDP parameters for unmilled As_xSe_{100-x} are pointed out by red circles on Figures 5 and 6. The high-energy MM does not change the principal character of these dependences, but changes in the values of the above parameters are notable, especially in some compositional domains. Thus, in the milled under-stoichiometric As_xSe_{100-x} ($5 \le x \le 40$), the FSDP position Q_1 (black-square pointed in Figure 5A) and, correspondingly, the spacing of the FSDP-responsible periodicity R (black-square pointed in Figure 6A) remains nearly the same as before milling (red-circle pointed in Figures 5, 6). Conversely, the FSDP width ΔQ_1 is slightly enhanced (Figure 5B) and correlation length L is reduced (Figure 6B) in milled As_xSe_{100-x} glasses with $20 \le x \le 40$.

In over-stoichiometric As_xSe_{100-x} ($40 \le x \le 65$), the effect of high-energy MM is evidently more pronounced, and surprisingly unexpected. Indeed, in this compositional range, the unmilled glasses show strong deviations towards lower Q_1 values (black-square pointed in Figure 5A), as it could be expected from linear $Q(x)$ dependence extrapolated for under-stoichiometric As_xSe_{100-x} ($5 \le x \le 40$):

$$Q = 1.45–4.45 \cdot 10^{-3} \cdot x. \quad (6)$$

The high-energy MM initiates partial recovery of the FSDP positions in over-stoichiometric glassy As-Se (red-circle pointed in Figure 5A) towards extrapolated line, this effect being inessential near the border of glass-forming region in As_xSe_{100-x} system at high As content ($x > 65$). The most pronounced relative deviations from this extrapolated $Q(x)$ line depicted in Figure 7 are characterized for unmilled $As_{50}Se_{50}$ and $As_{55}Se_{45}$ glasses ($\delta Q/Q_0$ ~8%), as well as milled $As_{55}Se_{45}$ and $As_{60}Se_{40}$ glasses ($\delta Q/Q_0$ ~4%). These changes in over-stoichiometric As_xSe_{100-x} glasses can be presented by plotting the spacing of the FSDP-responsible periodicity R against x parameter, as illustrated in Figure 6A.

As for the FSDP width ΔQ_1, this parameter shows most substantial changes in the milled over-stoichiometric As_xSe_{100-x} glasses with x stretching up to the border of glass-forming region (Figure 5B). The similar but evidently smaller changes are proper to milled Se-rich glasses ($20 \le x \le 40$) shown in Figure 5B. The correlation lengths L determined from ΔQ_1 using Equation (4) are reduced after MM as compared with unmilled over-stoichiometric As-rich As-Se glasses (see Figure 6B). Thus, for instance, the L approaches are ~37 and ~18 Å in unmilled and milled $As_{60}Se_{40}$ glass, respectively.

These MM-driven changes in the FSDP are completely concomitant with changes in the PDP. The PDP position Q_2 and width ΔQ_2 remain unchanged in milled Se-rich arsenoselenide glasses, while, in As-rich As-Se glasses, both parameters are kept after milling at the level more closer to As_2Se_3 (Figure 8). Thereby, increasing Q_2 and decreasing ΔQ_2 tendencies in under-stoichiometric As_xSe_{100-x} glasses with x parameter are hidden in the milled As-rich glasses.

It is worth noting that there are no detectable changes in the TDP-related XRPD patterns in As_xSe_{100-x} glasses (at ~50-60 $^o2\Theta$ or Q ~3.3-4.0 $Å^{-1}$) with glass composition and milling state. So

it seems reasonable assuming that structural entities responsible for compositional variation in diffuse halos (FSDP and PDP) in the XRPD patterns of over-stoichiometric As-Se glasses are merely destroyed under MM, keeping the medium-range structure of these glasses similar to As_2Se_3.

3.3 Microcrystallinity impact on MM-derived medium-range ordering in glassy As-Se

In general opinion, the FSDP is accepted as a direct manifestation of intermediate-range ordering in a glass,[14] despite a lot of controversies concerning microstructural origin of this diffuse peak-halo in XRPD patterns of many glasses.[39, 40] Chronologically, one of the first was the *microcrystalline* model alternatively termed as the *distorted-layer (molecular)* model, originally proposed by Vaipolin and Porai-Koshits yet in the earliest 1960s,[41] who treated diffuse halos (incl. the FSDP) in glasses due to remnants of distorted (quasi-crystalline) structures proper to their crystalline counterparts.[42] It was suggested that stacked *covalent-bonded molecular*—and/or *layer-type network-forming entities* with correlated inter-planar distances of R ~5-6 Å proper to crystalline chalcogenides were kept in glassy state, while layers themselves are highly corrugated, waved and distorted ensuring spatially restricted stacking domains of ~20-30 Å.

In fact, this approach was further developed in the Gaskel's concept on crystalline-like ordering in melt-quenched glasses[43] modified by Wright's justification[44] on the FSDP as arising from periodicity (quasi-periodicity) in distribution of some pseudo-planes for Bragg diffraction separating succession of randomly packed network cages. In respect to this *microcrystalline concept*, the flattened cage-like structure of network glasses produces inner equivalent planes at the opposite sides of these cages, forming a necessary contribution to the FSDP-generation reciprocal space Fourier component. Thus, the FSDP can be ascribed to variations in the underlying cage structure of glass-forming networks composed by interlinked polyhedrons (network-forming blocks), producing a variety of interlinked circle-type entities (small rings), keeping some elements of inter-planar ordering proper to crystalline counterparts of these glasses. This standpoint occurred to be very useful in the interpretation of *crystalline-to-amorphous* transitions in many arsenic compounds (arsenicals) subjected to high-energy MM.[45-47]

Within this approach applied to under-stoichiometric As_xSe_{100-x} glasses ($5 \le x \le 40$), the FSDP can be ascribed to structural networks built of trigonal $AsSe_{3/2}$ pyramids interlinked by Se-chains, ie inter-planar order proper to crystalline As_2Se_3 with character 12-membered corrugated rings,[9, 48-50] disturbed by $(\text{-Se-Se-})_n$ chains of different lengths n (in dependence on the glass composition).

The governing role of quasi-crystalline *inter-planar correlations* in the XRPD halos of As_2Se_3 glass is credibly confirmed by close similarity with angular positions of Bragg-diffraction reflexes attributed to its main crystalline homolog, ie the layer-type As_2Se_3,[48-50] as shown in Figure 9A. Remarkable coincidence between the positions and shapes of diffuse halos and grouped sets of most pronounced Bragg-diffraction reflexes is evident, despite the high-angular shift in (020) inter-layer spacing corresponding to R ~4.95 Å.[18, 19] The latter is expected for vitreous solids as compared with their crystalline homologs due to difference in their densities.[51, 52] Thus, the density of crystalline[48, 49] As_2Se_3 ρ^{cr} ~4.85 g·cm^{-3} is lowered in As_2Se_3 glass[11] on nearly ~5% reaching ρ^{g} ~4.605 g·cm^{-3}.

With Se additions to stoichiometric As_2Se_3 glass, the FSDP-responsible inter-planar ordering does not change essentially. The higher content of homonuclear Se-Se bonds in glassy network, which

are shorter than heteronuclear As-Se ones ($l_{Se\text{-}Se} \cong 2.32$ Å and $l_{As\text{-}Se} \cong 2.43$ Å),[9, 10] leads to the shorter nearest-neighbor inter-atomic distance d_s, and, consequently, the smaller periodicity R (see Figure 6A), while the correlation length L decreases slightly (as illustrated by Figure 6B). The broadened Bragg-diffraction reflexes of trigonal Se, especially the strongest ones originated from (101) and (100) planes corresponding to inter-planar distances d of ~3.01 and ~3.78 Å, respectively,[18, 19, 53] are both fit rather in angular range of the PDP than the FSDP (see Figure 9A), thus occurring more influence on extended-range than intermediate-range structural ordering.

Reasonably, these changes are accompanied by dropping in the FSDP intensity with Se excess, this effect being accompanied by evident L increase when going over a barrier of ~80 at. Se % in $As_{20}Se_{80}$ (Figure 6B), corresponding to eutectic in the phase diagram of As-Se system.[9, 54, 55] The latter can be assumed as resulting from appearance of another structural arrangement in this compositional domain, this being the network of Se-chains composed of Se atoms in preferential *trans*-configurations, and Se-rings built of Se atoms in *cis*-configurations.[9, 50] Thereby, the FSDP reduction in under-stoichiometric As-Se when going towards to "pure" Se as arising from disappearance of cation-cation correlations related to this peak can be accepted.[30, 31] From inspecting Figures 5 and 6, it seems that MM does not influence the FSDP-responsible correlations in proximity to glassy Se. In contrast, a slight increase in the FSDP width ΔQ_1 for As_xSe_{100-x} with $20 \le x \le 40$ can be ascribed to reduction in the correlation length L due to defects generated under MM, which disturb the FSDP-responsible inter-planar correlations due to mechanically built-in stresses. This range in As-Se system is known to be full of some instabilities, tending to local decomposition on As- and Se-rich fragments and/or global separation on As_2Se_3- and Se-rich arsenoselenide phases,[56] occurring fragmentation effect on the correlation length L of the FSDP-responsible quasi-periodicity.

Within the microcrystalline approach applied to over-stoichiometric glassy As_xSe_{100-x} ($40 \le x \le 65$) and mixed crystalline-amorphous $As_{70}Se_{30}$ and $As_{75}Se_{25}$ alloys, the FSDP can be considered as arising mainly from remnants of crystalline *cage-like* molecular structures proper to As-rich arsenoselenides, particularly, monoclinic[48] As_4Se_4 and orthorhombic[57] As_4Se_3, in addition to layer-type structure of corner-sharing $AsSe_{3/2}$ pyramids proper to monoclinic[48-50] As_2Se_3. Glass-forming network derivatives of realgar-type As_4Se_4 molecules are expected to dominate in this compositional range, as it follows from $\delta Q/Q_0$ dependence as shown in Figure 7 showing strong maximum just near this composition. So the FSDP-responsible cation-cation correlations are substantially enhanced with As content in As-Se glasses resulting in increased intermediate-range structural ordering.[30] This compositional trend is accompanied by shifts in the FSDP position towards lower 2Θ (see Figure 9), because of overlapping with broadened Bragg-diffraction reflexes of some remnants of molecular phases, in part, arising from (120) plane of monoclinic As_4Se_4 at ~16.07 $^o2\Theta$ (d = 5.51 Å, 91.26%)[18, 19, 48] and (111) plane of orthorhombic As_4Se_3 at ~16.90 $^o2\Theta$ (d = 5.24 Å, 100%).[18, 19, 57] These phases cause only slight effect on the PDP. Indeed, reflexes from molecular As_4Se_3 remnants are depressed in this 2Θ range, (below 66% in intensity),[57] while strong reflexes of As_2Se_3, As_4Se_4 and As phases are compactly grouped near ~32 $^o2\Theta$ (Figure 10), these respectively arising from (311) plane at ~31.91 $^o2\Theta$ (d = 2.80 Å), (141) plane at ~32.17 $^o2\Theta$ (d = 2.78 Å) and (012) plane at ~32.29 $^o2\Theta$ (d = 2.77 Å).[18, 19, 48, 49, 57]

The primary effect of MM on over-stoichiometric As-Se can be imagined as the destruction of these circle-type entities to form more chain-like networks, the milled glasses behaving as those with

more reduced As content. Thus, the FSDP position Q_1 is evidently enhanced (Figure 5A) and, respectively, the spacing of the FSDP-responsible quasi-periodicity R is reduced (Figure 6A) with maximal effect reaching −3.2% for milled $As_{60}Se_{40}$. These changes are accompanied by gradual broadening in the FSDP width ΔQ_1 (Figure 5B), resulting in dramatically reduced L (Figure 6B) beyond 40% for milled As-rich As_xSe_{100-x} glasses ($45 < x < 75$). Thus, the high-energy MM causes *fragmentation* impact on the correlation length L of quasi-periodic structural entities responsible for the FSDP in these glasses.

Principally, the MM-driven destruction of intermediate-range ordering in glassy As-Se revealed through the FSDP means changed role of the extended-range ordering determined by the PDP at ~28-36 $^{o}2\theta$ (or, alternatively, the SSDP).[14, 37, 58, 59] But in under-stoichiometric Se-rich As_xSe_{100} ($5 \le x \le 40$), these changes are rather negligible, testifying in a favor of structural transformations completely dominated in intermediate-range ordering, as it occurs in some molecular chalcogenide glasses under moderated pressure-induced densification.[60, 61] In contrast, in the milled As-rich glasses ($40 \le x \le 65$), drastic effects in the FSDP are counterbalanced by changes in the PDP. Thus, the PDP position for glasses with $x > 55$ shifts to higher scattering vectors Q_2 after MM (over 4.0% in relative determination), this peak getting more broadened in a width ΔQ_2 (over 20%).

Noteworthy, similar interrelations between the FSDP and PDP were also observed by De Neufville et al[24] in the XRD patterns of as-deposited As_2Se_3 films (thickened to 22 μm), affected by thermal annealing below glass-transition temperature or illuminated by absorbed light. Such changes were also detected by Sarsembinov et al[27] in As_2Se_3 films (having 4-12 μm in a thickness) prepared by thermal evaporation in vacuum and ion-plasma sputtering.

3.4 Modified microcrystalline approach to MM-derived medium-range ordering in As-Se

The above interpretation of MM-induced structural transformations in glassy As_xSe_{100-x} is developed accepting diffuse halos in their XRPD patterns as arising predominantly from overlapped broadened Bragg-diffraction reflexes of compositionally close crystalline remnants in their networks. Detailed analysis of the XRPD patterns (Figures 1-3, 9) testifies that such an approach alone, grounded exceptionally on *inter-planar Bragg-diffraction correlations* of homological crystals is insufficient to explain all details in the underlying *medium-range structural ordering* in As-Se.

More straightforward interpretation of compositional variations in the XRPD patterns of As-Se glasses can be developed within *modified microcrystalline approach*, accepting their diffuse halos as superposition of broadened Bragg-diffraction reflexes from remnants of microcrystalline *inter-planar correlations R*, supplemented by diffuse halos from prominent *pair inter-atomic correlations* d_s, ie diffuse halos originated from coordination spheres obeying the Ehrenfest relation (5). The latter is known to be a useful approach to treat the XRPD patterns of *ideal amorphous solids*, which can be characterized by structures composed of randomly positioned hard contacting spheres, obeying ideal dense-random-packing (DRP) arrangement.[24, 26, 34, 35]

In a glassy state, the Ehrenfest diffraction from inter-atomic correlations is merely hidden as compared with Bragg diffraction from inter-planar (inter-layer) correlations.[35] Nevertheless, it can be reasonably accepted that XRPD patterns are essentially disturbed in covalent-bonded network As-Se glasses by superposition from the Ehrenfest-diffraction reflexes. In the first hand, it concerns

an *anomalous behavior* of the FSDP under external influences such as applied pressure or temperature,[42, 62-64] which can be ascribed to overlapping with inter-atomic correlations, possessing principally different responses on external distortions. Thus, in respect to known pair correlation functions for glassy As-Se,[65, 66] two pronounced inter-atomic distances d_S are fit in angular diffraction domain of the FSDP in dependence on the glass composition, these being close to ~6 and ~7 Å. For example, in the structure of glassy As_2Se_3, the dominated d_S approaching ~5.8 and ~6.9 Å terminated by deep depopulation regions are detected (as it is demonstrated by Renninger et al[65]). A shorter d_S is expected for right-sided FSDP wing (at higher diffraction angles 2θ), while the longer one is proper to left-sided wing (at lower 2θ). In As-Se glasses, these distances d_S correspond to lengths between cation-like atoms belonging to extended structural entities such as layers (quasi-layers) or molecules (quasi-molecules), forming third-order (As)–(As) pair correlations.[30, 31, 37, 38, 42, 62]

Such inter-atomic pairs between neighboring sheets separated by (020) plane can be visualized in the monoclinic lattice of As_2Se_3 exploring the DIAMOND program,[20] the respective computed view with some distinguished (As)–(As) distances are being shown in Figure 10. The denoted pairs represent *inter-atomic correlations* (subject to the Ehrenfest diffraction) in glassy $As_{40}Se_{60}$ close to ~4.95 Å, ie the distance between (020) planes (subject to the Bragg diffraction). These distances are somewhat enhanced owing to almost ~5% dropping in the glass density respectively to the crystal.[9, 51, 52] Because of *asymmetric arrangement* of such inter-atomic correlations contributing to the FSDP in respect to the closest inter-planar correlation (Figure 10), the corresponding halo demonstrates an anomalous response on external influences, when some inter-atomic distances belonging to these sheets do not change intact (if one grows, the other shortens, and vice versa).

In general, a similar scenario is expected for molecular substances, where such misbalanced inter-atomic correlations are revealed in *asymmetric linkages* between neighboring quasi-molecules. Thus, Figure 11 provides visualization of a few As_4Se_4 molecules in the structure of monoclinic As_4Se_4. For As atoms chosen within one As_4Se_4 molecule, the third-order inter-atomic distances with other atoms belonging to neighboring As_4Se_4 molecules, which are over- and under-estimated in respect to inter-molecular centroid-centroid B-B distance, can be simply visualized. These inter-atomic (As)–(As) pairs are *asymmetrically arranged*, ensuring anomalous response on lattice distortions, like in previous case of quasi-layered structures.

In a reasonable accord to the above consideration, we believe that the FSDP in As_xSe_{100-x} glasses observed at Q_1 ~1.42-1.10 $Å^{-1}$ can be attributed to commensurable contributions from *inter-planar correlations* due to crystalline remnants of close compositions with Bragg-diffraction distances R = 4.41-5.72 Å, and *inter-atomic correlations* due to third-order (As)–(As) pairs with averaged distances of d_S = 5.42-7.05 Å (the numerical values are given in a sequence of increased As content).

The nonelementary nature of diffuse halos in chalcogenide glasses revealed through more or less pronounced features (humps, asymmetric extensions, “tails”) serves as one of the most conclusive arguments evidencing contribution of Ehrenfest diffraction from *pair inter-atomic correlations* d_S.

On the first hand, this concerns the post-FSDP (shoulder observed at high-angular side of the FSDP in many chalcogenide glasses as summarized by Popescu).[67] This feature was often ignored, being ascribed to uncertainties in the XRPD measurements. But sometimes direct indicatives on broadened FSDP superimposed on weak right-sided satellite hump were pointed out for some

glasses showing pronounced FSDP.[67-69] Thus, a distinct shoulder at Q ~1.7 $Å^{-1}$ was observed in $As_2(S/Se)_3$ by Mori et al[70]. An asymmetric FSDP broadening was detected in As_2S_3 under photoexposure by K. Tanaka.[71, 72] In our XRPD study, the post-FSDP shoulders, despite not being reproducible in the structure factor $S(Q)$ (Figure 4), were detected in all As_xSe_{100-x} samples from their glass-forming region ($5 \le x \le 65$). Analysis shows that positions of these respective peak features.

$$k\ (FSDP) = Q^{post-FSDP} / Q^{FSDP} \quad (7)$$

Can be well rationed as close to the Ehrenfest number 1.23.34

Similar peculiarities can be found on XRPD patterns in a vicinity of the PDP (~28-33 $^{o}2\Theta$, see Figures 2-4, 10). Additional satellite peak (reasonably referred to as the post-PDP) located at right-sided tail can be fitted to this diffuse halo to justify its asymmetric shape. Noteworthy, in this case, the relation similar to the above (7) can be evidenced as being close to the Ehrenfest number 1.23:

$$k\ (PDP) = Q^{post-PDP} / QP^{DP} \quad (8)$$

Therefore, we can reasonably speculate that asymmetry in the PDP can be caused by superposition of broadened Bragg-diffraction reflexes from inter-planar correlations (due to remnants of some quasi-crystalline planes) superimposed by Ehrenfest-diffraction reflexes from most prominent correlations between some atomic pairs belonging to these planes.

It is worth mentioning that the doublet nature of the TDP at ~50-60 $^{o}2\Theta$ associated with direct nearest-neighbor separation in chalcogenide glasses (see Figures 2, 9) is rather unrevealed.[28] Contribution from Ehrenfest-diffraction reflexes is expected on left-sided wing of this halo for closest nearest-neighbor correlations caused by covalent bonds in As-Se glasses.

Secondly, the Ehrenfest diffraction seems to be most suitable approach explaining other anomaly in the XRPD patterns of chalcogenide glasses known as pre-FSDP,[67, 73-76] (viz. additional peak-halo at low diffraction angles of ~5-7 $^{o}2\theta$, ie in the region where there are no inter-planar Bragg-diffraction reflexes from possible crystalline counterparts). The diffuse halo in this angular domain can be explained as arising from more *prolonged inter-atomic correlations* in a glass approaching d_s ~15-20 Å. Like post-FSDP, this feature is also unreproducible in the structure factor $S(Q)$ (Figure 4).

Thus, we conclude on reasonable necessity to parameterize the XRPD patterns in As-Se glasses accepting their diffuse halos as originated from superimposed *inter-planar* (R) and *inter-atomic* (d_s) correlations. It means that both low-angular diffuse peaks (the FSDP and PDP) should be considered as composed of two distinct ones (doublet of halos), these being the main low-Q peak and satellite high-Q postpeak (the post-FSDP and post-PDP). The results of such decomposition for some representative unmilled and milled As_xSe_{100-x} samples (x = 40, 50, 60) are gathered in Table 1.

Table 1. Peak halos-related correlations in unmilled and milled over-stoichiometric As_xSe_{100-x} accepting decomposition procedure with distinct post-FSDP and post-PDP components

Sample, state:		**Peak-halo's parameterization**				
κ(FSDP), κ(PDP)	**Peak-halo**	***Q*** **$Å^{-1}$**	***ΔQ*** **$Å^{-1}$**	***R*** **Å**	***L*** **Å**	***d*** **$_s$** **Å**
	Pre-FSDP	0.438	0.308	14.3	20.4	17.6

Sample, state: ***κ*(*FSDP*), *κ*(*PDP*)**	**Peak-halo**	**Peak-halo's parameterization**				
		Q **Å^{-1}**	***ΔQ*** **Å^{-1}**	***R*** **Å**	***L*** **Å**	d_s **Å**
$As_{40}Se_{60}$, unmilled:	FSDP	1.234	0.362	5.1	17.3	6.3
	Post-FSDP	1.490	0.561	4.2	11.2	5.2
κ(*FSDP*) = 1.21	PDP	2.227	0.514	2.8	12.2	3.5
κ(*PDP*) = 1.19	Post-PDP	2.653	0.339	2.4	18.5	2.9
	TDP	3.641	0.620	1.7	10.1	2.1
$As_{40}Se_{60}$, dry-milled:	Pre-FSDP	0.432	0.334	14.5	16.9	17.5
	FSDP	1.214	0.304	5.2	16.9	6.4
κ(*FSDP*) = 1.26	Post-FSDP	1.525	0.492	4.1	12.8	5.1
	PDP	2.210	0.511	2.8	12.3	3.5
κ(*PDP*) = 1.16	Post-PDP	2.555	0.447	2.5	14.1	3.0
	TDP	3.635	0.636	1.7	9.9	2.1
$As_{50}Se_{50}$, unmilled:	Pre-FSDP	0.443	0.285	14.2	22.0	17.4
	FSDP	1.138	0.228	5.5	27.5	6.8
κ(*FSDP*) = 1.24	Post-FSDP	1.414	0.302	4.4	20.8	5.5
	PDP	2.096	0.419	3.0	15.0	3.7
κ(*PDP*) = 1.13	Post-PDP	2.378	0.503	2.6	12.5	3.3
	TDP	3.617	0.624	1.7	10.1	2.1
$As_{50}Se_{50}$, dry-milled:	Pre-FSDP	0.442	0.334	14.2	18.8	17.5
	FSDP	1.165	0.304	5.4	20.7	6.6
κ(*FSDP*) = 1.26	Post-FSDP	1.473	0.258	4.3	24.3	5.2
	PDP	2.171	0.500	2.9	12.6	3.6
κ(*PDP*) = 1.16	Post-PDP	2.512	0.456	2.5	13.8	3.1
	TDP	3.632	0.631	1.7	10.0	2.1
$As_{60}Se_{40}$, unmilled:	Pre-FSDP	0.468	0.340	13.4	18.5	16.5
	FSDP	1.107	0.188	5.7	33.4	7.0
κ(*FSDP*) = 1.38	Post-FSDP	1.530	0.019	4.1	329	5.1
	PDP	2.061	0.370	3.0	17.0	2.3
κ(*PDP*) = 1.15	Post-PDP	2.378	0.527	2.6	12.1	3.2
	TDP	3.590	0.637	1.7	10.0	2.1
$As_{60}Se_{40}$, dry-milled:	Pre-FSDP	0.440	0.358	14.3	17.6	17.6
	FSDP	1.143	0.324	5.5	19.4	6.8
κ(*FSDP*) = 1.34	Post-FSDP	1.530	0.170	4.1	37.0	5.1
	PDP	2.136	0.446	2.9	14.1	3.6
κ(*PDP*) = 1.11	Post-PDP	2.379	0.527	2.6	11.9	3.2
	TDP	3.623	0.627	1.7	10.0	2.1

It is clearly seen the pre-FSDP does not demonstrate essential and reproducible effects under changing in As-Se glass composition, as well as under high-energy MM (see Figure 9). The pre-FSDP position remains invariant around mean inter-atomic distance of d_s = 17.5 Å (small deviation in unmilled $As_{60}S_{40}$ seems accident). The similar behavior is also character for TDP positioned in all samples in a vicinity of Q reaching ~3.6 Å^{-1} (see Table 1).

As in the previous case treating each XRPD peak in glassy As_xSe_{100-x} as one distinct diffuse halo, the main low-*Q* FSDP-halo reveals an obvious tendency to be shifted towards higher scattering vectors *Q* accompanied by substantial increase in the width ΔQ, these changes being enhanced in As-rich arsenoselenide glasses (see Table 1). These effects were not strictly reproduced in the satellite high-*Q* post-FSDP, which remained tightly connected to main FSDP through Equation (7) with the numerical $\kappa(FSDP)$ ratio slightly above the Ehrenfest number. With MM, the most pronounced inter-atomic correlations d_S responsible for post-FSDP became reduced as compared with inter-planar correlations *R* ascribed to the FSDP, thus ensuring increased κ values in milled As-Se glasses (Table 1). It means that MM-driven breakdown in intermediate-range ordering is expended over destruction of most distant inter-atomic correlations belonging to remnants of crystalline planes contributing to the FSDP.

These changes are accompanied by more evident shifting in the position of main low-*Q* PDP towards higher *Q* values, and relatively moderated increase in the width of this peak-halo under MM (see Table 1). The post-PDP was further linked with main PDP through Equation (8) with (*PDP*) ratio, which was slightly reduced in respect to the Ehrenfest number, thus meaning that longer inter-atomic distances reaching 3.2 Å became most prominent in extended-range ordering of these glasses.

3.5 On the role of inter-molecular correlations in over-stoichiometric glassy arsenoselenides

The above model considering most prominent inter-atomic correlations in glassy As-Se belonging to inter-planar Bragg-diffraction entities (ie remnants of microcrystalline layer-type structures) does not explain compositional collapse in the FSDP-PDP parameterization in over-stoichiometric As-rich As-Se glasses as compared with stoichiometric As_2Se_3 and under-stoichiometric ones (Figure 9). As was convincingly proved by Yang et al,[13] the structure of over-stoichiometric arsenoselenides (like crystalline arsenic sulfides)[77] can be treated as stacking of *network-type entities* based on Se-linked $AsSe_{3/2}$ pyramids and cage-like As_4Se_4, As_4Se_3 and probably As_4 *molecular-type entities*. To visualize spatial stacking of such molecules, Bonazzi and Bindi[77] introduced “dummy atom” B for each molecule, treating it as geometrical barycenter. Such an approach allows estimation of the shortest inter-molecular centroid-centroid distances B-B in different molecular structures and their packing in some crystallographic planes.[77] From the point of diffuse halos in the XRPD patterns of glassy As-Se, another aspect of this routine seems very promising, namely the DRP of such molecular entities (inter-molecular correlations), contributing through the Ehrenfest diffraction. In case of close DRP, each molecule is surrounded by 12 neighbors forming a cubic or hexagonal octahedron (six molecules being placed within one plane, 3 molecules above and 3 molecules below this plane).

Fragment of As_4Se_4 crystal structure visualized on the basis of experimental data taken from Kyono[78] using DIAMOND and VESTA programs[20, 21] is shown in Figure 12. This presentation demonstrates all possible inter-molecular centroid-centroid distances *B-B*, packing of As_4Se_4 cage-like molecules as the $B[B_{11}]$ polyhedron together with family of (120) crystallographic planes corresponding to the hkl reflection (120) proper to this structural type. It is seen that each As_4Se_4 molecule is surrounded by 11 neighbors forming a $B[B_{11}]$ polyhedron, which can be considered as an incomplete distorted cubooctahedron with face-centered cubic close packing of Cu structure type (shown at the bottom left in Figure 12) and $d_{B\text{-}B}$ distances deviated from 5.778 to 7.734 Å. The

averaged d^{av}_{B-B} distance over a whole polyhedron approaches 6.728 Å. This distance accepted as the first coordination sphere in the DRP of As_4Se_4 cages obeying the Ehrenfest relation (5) remarkably fits with the FSDP position recalculated as Bragg-diffraction peak on the XRPD pattern of $As_{50}Se_{50}$ glass (see Figure 9B).

A similar situation is character for high-temperature As_4Se_3 crystal structure composed of iso-compositional cage-like molecules (see Figure 13). In this case, each As_4Se_3 molecule is surrounded by 12 neighbors, forming a $B[B_{12}]$ polyhedron, which can be considered as a deformed anticubooctahedron with hexagonal close packing of Mg structure type (shown at the bottom left in Figure 13) and *B-B* distances d_{B-B} deviated from 5.651 to 7.910 Å. The averaged d^{av}_{B-B} distance within this $B[B_{12}]$ polyhedron approaches 6.650 Å, also very close to the FSDP position in $As_{60}Se_{40}$ glass (see Figure 9C). These As_4Se_3 molecular units, which possess some orientation-rotational freedom in view of their spherical symmetry (all atoms constituting this molecule occupy nearly the same sphere)[57, 79] are responsible for extra rapid reduction in glass-transition temperature T_g in As-Se glasses at high As content. In some cases, when T_g values reach room temperature as in the second glass-forming region in As-S system,[80] the melt-quenched glasses of this type attain unusual plasticity.

Such *inter-molecular correlations* are believed to be revealed in over-stoichiometric As-Se glasses through Ehrenfest diffraction obeying relation (5), where average inter-atomic distance d_s is replaced by centroid-centroid *B-B* distance between densely packed As_4Se_4 and/or As_4Se_3 molecules. As a result, the FSDP is essentially narrowed in a width and highly enhanced with these contributions (in addition to inter-planar correlations from crystalline remnants of these arsenoseleniden Q_1 and width ΔQ_1, as it was demonstrated on Figure 5). The high-energy MM occurs destructive impact on these inter-molecular correlations, tending the structure of milled over-stoichiometric glassy As-Se towards network-like topology character for stoichiometric As_2Se_3 glass. This *reamorphization* effect in over-stoichiometric glassy arsenoselenides driven by MM results in substantially broadened and high-*Q* shifted FSDP (in full respect to the obtained experimental data as shown, eg, in Figure 9).s), its position Q_1 being stabilized in a very close vicinity to these d^{av}_{B-B} distances.

The question on topological identity of these molecular entities in over-stoichiometric arsenoselenide glasses is still remaining open. Indeed, the spatial positioning of barycenter *B* of As_4Se_4 (or As_4Se_3) molecules does not change substantially under partial polymerization of these molecules in glassy network, if some elements of these molecules such as small 3-, 4- and/or 5-folded circles are kept, as it was in the case of MM-driven amorphization in β-As_4S_4 polymorph.[46, 47] Appearance of such inter-molecular correlations between cage-like As_4Se_4 and As_4Se_3 molecules and their partially polymerized remnants in melt-quenched over-stoichiometric As-Se glasses leads to anomalous compositional behavior of the FSDP (drastic decrease in the FSDP position Q_1 and width ΔQ_1, as it was demonstrated on Figure 5). The high-energy MM occurs destructive impact on these inter-molecular correlations, tending the structure of milled over-stoichiometric glassy As-Se towards network-like topology character for stoichiometric As_2Se_3 glass. This *reamorphization* effect in over-stoichiometric glassy arsenoselenides driven by MM results in substantially broadened and high-*Q* shifted FSDP (in full respect to the obtained experimental data as shown, eg, in Figure 9).

4. CONCLUSIONS

Effect of high-energy dry MM on medium-range structural ordering of glassy As_xSe_{100-x} ($5 \le x \le 75$) is studied employing XRPD analysis applied to their diffuse halos ascribed to intermediate- and extended-range ordering, respectively revealed in the FSDP at the scattering vectors $Q_1 \cong$ ~1-1.5 $Å^{-1}$ and PDP at $Q_2 \cong$ ~1.9-2.3 $Å^{-1}$. Straightforward interpretation of the observed changes in the XRPD patterns is developed within *modified microcrystalline approach*, accepting diffuse halos in As-Se glasses as superposition of *inter-planar*- and *inter-atomic correlations* originated from remnants of some crystalline homologs. The sources of *inter-atomic correlations* contributing to the FSDP (the Ehrenfest diffraction) are *third-order As–As correlations* belonging to remnants of crystallographic planes forming most prominent Bragg-diffraction reflexes, and *inter-molecular correlations* between more extended entities, such as partially polymerized cage-like As_4Se_4, As_4Se_3 and/or As_4 molecules.

Under milling, the thermodynamically stabilized balance in network-forming entities in glassy As-Se is disturbed, providing evidence on defects with unfavorable energies. Milling does not influence the FSDP in Se-rich As_xSe_{100-x} ($x < 20$), but causes an increase in the FSDP width ΔQ_1 for glasses with $20 \le x \le 40$. This effect is ascribed to disturbed inter-planar ordering in these glasses due to generated defects. In over-stoichiometric As_xSe_{100-x} ($40 \le x \le 65$), the FSDP position Q_1 grows towards the line extrapolated from under-stoichiometric glasses, this effect being inessential at high As content. In contrast, the FSDP width ΔQ_1 shows pronounced enhancement with growing x. It is assumed that milling destroys remnants of cage-like molecules (As_4Se_4, As_4Se_3) promoting formation of chain-like network structures. Therefore, the milling-driven *reamorphization* results in a drastic increase in the FSDP position and width, producing the *fragmentation impact* on the correlation length ascribed to the FSDP-responsible entities. Destruction of intermediate-range ordering in the milled over-stoichiometric As-Se is accompanied by changes in their extended-range ordering, revealed in high-angular shift in the PDP position and broadening in the PDP width.

Assuming the doublet nature of the FSDP and PDP, the observed changes in the XRPD patterns of As-Se are ascribed to milling-induced destruction of some remnants of inter-planar and inter-molecular correlations proper to their crystalline homologs. Milling-driven changes in the intermediate-range ordering are concomitant with the destruction of most distant inter-atomic correlations belonging to quasi-crystalline planes contributing to the FSDP, while longer inter-atomic correlations (~3.2 Å) become dominant in their extended-range ordering.

ACKNOWLEDGMENTS

This work was supported by the Slovak Research and Development Agency under the contract no. APVV-18-0357 and POLONIUM common action program for years 2018-2019 realized in respect to bilateral Agreement on scientific-technical cooperation between Polish and French governments.

REFERENCES

1. Ajayan PM, Schadler LS, Braun PV. Nanocomposite science and technology. Weinheim: Wiley-VCH Verlag GmbH & Co. KgaA; 2003.

2. Baláž P. Mechanochemistry in nanoscience and minerals engineering. Berlin-Heidelberg: Springer; 2008.

3. Baláž P, Achimovicova M, Baláž M, Billik P, Cherkezova-Zheleva Z, Manuel Criado J, et al. Hallmarks of mechanochemistry: from nanoparticles to technology. Chem Soc Rev. 2013;42:7571–637.

4. Keddie JL, Jones RA, Cory RA. Size-dependent depression of the glass transition temperature in polymer films. Europhys Lett. 1994;27(1):59–64.

5. Keddie JL, Jones RA, Cory RA. Interface and surface effects on the glass-transition temperature in thin polymer films. Faraday Disscuss. 1994;98:219–30.

6. Ellison CJ, Torkelson JM. The distribution of glass-transition temperatures in nanoscopically confined glass formers. Nat Mater. 2003;21:695–700.

7. Salez T, McGraw JD, Dalnoki-Veress K, Raphael E, Forrest JA. Glass transition at interfaces. Europhys News. 2017;48(1):24–8.

8. Cangialosi D, Alegria A, Colmenero J. Effect of nanostructure on the thermal glass transition and physical ageing in polymer materials. Progr Polym Sci. 2016;54–55:128–47.

9. Feltz A. Amorphous inorganic materials and glasses. Weinheim: VCH; 1993.

10. Feltz A, Aust H, Blayer A. Glass formation and properties of chalcogenide systems XXVI: permittivity and the structure of glasses AsxSe1-x and GexSe1-x. J Non-Cryst Solids. 1983;55:179–90.

11. Shpotyuk Y,Boussard-Pledel C, BureauB,Demchenko P,SzlęzakJ,Cebulski J, et al.Effect of high-energy mechanical milling on the FSDP-related XRPD correlations in Se-rich glassy arsenic selenides. J Phys Chem Solids. 2019;124:318–26.

12. Adam J-L, Zhang X, editors. Chalcogenide glasses: preparation, properties and application. Philadelphia-New Delhi: Woodhead Publ. Series in Electronic and Optical Materials; 2013.

13. Yang G, Bureau B, Rouxel T, Gueguen Y, Gulbiten O, Roiland C, et al. Correlation between structure and physical properties of chalcogenide glasses in the AsxSe1−x system. Phys Rev B. 2010;82:195206-1-8.

14. Elliott SR. Extended-range order, interstitial voids and the first sharp diffraction peak of network glasses. J Non-Cryst Solids. 1995;182:40–8.

15. Stoe WinXPOW (version 3.03). Darmstadt: Stoe & Cie GmbH; 2010.

16. Egami T, Billinge SJL. Underneath the bragg peaks. Structural analysis of complex materials. Vol. 16, 2nd ed. Oxford, Amsterdam, San Diego: Pergamon; 2013.

17. Qiu X, Thompson JW, Billinge SJL. PDFgetX2: a GUI driven program to obtain the pair distribution function from X-ray powder diffraction data. J Appl Cryst. 2004;37:678.

18. Downs RT, Hall-Wallace M. The American mineralogist crystal structure database. Am Mineral. 2003;88:247–50.

19. Villars P, Cenzual K, editors. Pearson's crystal data: crystal structure database for inorganic compounds, Release 2014/15. Materials Park, OH: ASM International; 2014.

20. Brandenburg K. DIAMOND 3.2g, crystal and molecular structure visualization. Bonn: Crystal impact GbR; 2011.

21. Momma K, Izumi F. VESTA 3 for three-dimensional visualization of crystal, volumetric and morphology data. J Appl Crystallogr. 2011;44:1272–6.

22. Roisnel T, Rodriguez-Carvajal J. WinPLOTR: a Windows tool for powder diffraction patterns analysis. Mater Sci Forum. 2001;118:378–81.

23. Kraus W, Nolze G. POWDER CELL – a program for the representation and manipulation of crystal structures and calculation of the resulting X-ray powder patterns. J Appl Cryst. 1996;29:301–3.

24. De Neufville JP, Moss SC, Ovshinsky SR. Photostructural transformations in amorphous As2Se3 and As2S 3 films. J Non-Cryst Solids. 1974;13(2):191–223.

25. Wright AC, Sinclair RN, Leadbetter AJ. Effect of preparation method on the structure of amorphous solids in the system As-S. J Non-Cryst Solids. 1985;71:295–302.

26. Moss SC, Price DL. Random packing of structural units and the first sharp diffraction peak in glasses. In: Adler D, Fritsche H, Ovshinsky SR, editors. Physics of disordered materials. New York, London: Plenum Publishing Corporation, 1985; p. 77–95.

27. Sarsembinov ShSh, Prikhodko OYU, Ryaguzov AP, Maksimova SYA, Ushanov VZH. Atomic structure and short- and medium-range order parameters in amorphous chalcogenide films prepared by different methods. J Non-Cryst Solids. 2007;353:2057–61.

28. Zeidler A, Salmon PS. Pressure-driven transformation of the ordering in amorphous network-forming materials. Phys Rev B. 2016;93:214204-1-5.

29. Salmon PS. Real space manifestation of the first sharp diffraction peak in the structure factor of liquid and glassy materials. Proc R Soc London A. 1994;445:351–65.

30. Bychkov E, Benmore CJ, Price DL. Compositional changes in the first sharp diffraction peak in binary selenide glasses. Phys Rev B. 2005;72:172107-1-4.

31. Golovchak R, Lucas P, Oelgoetz J, Kovalskiy A, York-Winegar J, Saiyasombat CH, et al. Medium range order and structural relaxation in As–Se network glasses through FSDP analysis. Mater Chem Phys. 2015;153:432–42.

32. Bletry J. Sphere and distance models for binary disordered systems. Phil Mag B. 1990;62:469–508.

33. Sozin YUI. Diffractometry of coordination spheres. Crystallogr Rep. 1994;39:6–13.

34. Rachek OP. X-ray diffraction study of amorphous alloys Al-Ni-Ce-Sc with using Ehrenfest's formula. J Non-Cryst Solids. 2006;352:3781–6

35. Feng R, Stachurski ZH, Rodrigues MD, Kluth P, Araujo LL, Bulla D, et al. X-ray scattering from amorphous solids. J Non-Cryst Solids. 2013;383:21–7.

36. Ehrenfest P. On interference phenomena to be expected when Roentgen rays pass through a diatomic gas. Proc KNAW. 1914-1915;17:1184–90.

37. Elliott SR. Second sharp diffraction peak in the structure factor of binary covalent network glasses. Phys Rev B. 1995;51:8599–601.

38. Lukyanov A, Lubchenko V. Amorphous chalcogenides as random octahedrally bonded solids: I. Implications for the first sharp diffraction peak, photodarkening, and Boson peak. J Chem Phys. 2017;147:114505-1-20.

39. Shatnawi MTM. The first sharp diffraction peak in the total structure function of amorphous chalcogenide glasses: anomalous characteristics and controversial views. New J Glass Ceram. 2012;6:37–46.

40. Crupi C, Carini G, Ruello G, D'Angello G. Intermediate range order in alkaline borate glasses. Phil Mag. 2016;96:788–99.

41. Vaipolin AA, Porai-Koshits EA. Structural models of glasses and the structures of crystalline chalcogenides. Sov Phys Solid State. 1963;5:497–500.

42. Tanaka K, Shimakawa K. Amorphous chalcogenide semiconductors and related materials. New York, Dordrecht, Heidelberg, London: Springer; 2011.

43. Gaskell PH. The structure of simple glasses: randomness or pattern the debate goes on. Glass Phys Chem. 1998;24:180–7.

44. Wright AC. Crystalline-like ordering in melt-quenched network glasses? J Non-Cryst Solids. 2014;401:4–26.

45. Shpotyuk O, Kozdras A, Demchenko P, Shpotyuk Y, Bujňáková Z, Baláž P. Solid-state amorphization of As 45S55 alloy induced by high-energy mechanical milling. Thermochim Acta. 2016;642:59–66.

46. Baláž P, Baláž M, Shpotyuk O, Demchenko P, Vlček M, Shopska M, et al. Properties of arsenic sulphide (β-As4S4) modified by mechanical activation. J Mater Sci. 2017;52:1747–58.

47. Shpotyuk O, Baláž P, Bujňáková Z, Ingram A, Demchenko P, Shpotyuk Y. Mechanochemically-driven amorphization of nanostructurized arsenicals, the case of β-As 4S4. J Mater Sci. 2018;53:13464–76.

48. Renninger AL, Averbach BL. Crystalline structures of As2Se3 and As 4Se4. Acta Cryst B. 1973;29:1583–9.

49. Stergiou AC, Rentzeperis PJ. The crystal structure of arsenic selenide, As2Se3 . Zeitsch Krist. 1985;173:185–91.

50. Popescu MA. Non-crystalline chalcogenides. Dortrecht: Kluwer Academic Publishers; 2000.

51. Leadbetter AJ, Apling AJ. Diffraction studies of glass structure. J Non-Cryst Solids. 1974;15:250–68.

52. Bisaro R, Magarino J, Pastol Y, Germain P, Zellama K. Transient solid-phase crystallization study of chemically vapor-deposited amorphous silicon films by in situ X-ray diffraction. Phys Rev B. 1989;40:7655–62.

53. Cherin P, Unge14. Elliott SR. Extended-range order, interstitial voids and the first sharp diffraction peak of network glasses. J Non-Cryst Solids. 1995;182:40–8.

54. Blachnik R, Hoppe A, Wickel U. Die Systeme Arsen-Schwefel und Arsen-Selen und die thermodynamischen Daten ihrer Verbindungen. Z Anorg Allg Chem. 1980;463:78–90.

55. Myers MB, Felty EJ. Structural characterizations of vitreous inorganic polymers by thermal studies. Mater Res Bull. 1967;2:535–46.

56. Shpotyuk O, Hyla M, Boyko V. Compositionally-dependent structural variations in glassy chalcogenides: The case of binary As-Se system. Comput Mater Sci. 2015;110:144–51.

57. Bastow TJ, Whitfied HJ. Crystal data and nuclear quadrupole resonance spectra of tetra-arsenic triselenide. J Chem Soc Dalton Trans. 1977;1977:959–61.

58. Salmon PS, Martin RA, Mason PE, Cuello GJ. Topological versus chemical ordering in network glasses at intermediate and extended length scales. Nature. 2005;435:75–8.

59. Salmon PS, Barnes AC, Martin RA, Cuello GJ. Glass fragility and atomic ordering on the intermediate and extended range. Phys Rev Lett. 2006;96:235502-1-4.

60. Mei Q, Benmore CJ, Hart RT, Bychkov E, Salmon PS, Martin CD, et al. Topological changes in glassy GeSe2 at pressures up to 9.3 GPa determined by high-energy X-ray and neutron diffraction measurements. Phys Rev B. 2006;74:014303-1-10.

61. Soyer Uzun S, Gaudio SJ, Sen S, Mei Q, Benmore CJ, Tulk CA, et al. In situ high-pressure X-ray diffraction study of densification of a molecular chalcogenide glass. J Phys Chem Solids. 2008;69:2336–40.

62. Tanaka K. Chalcogenide glasses. In: K.H.J. Buschow, R. Cahn, M. Flemings, B. Ilschner, E. Kramer, S. Mahajan& P. Veyssiere (Eds.), Reference module in materials science and materials engineering. Encyclopedia of Materials: Science and Technology. 2nd ed. Amsterdam, the Netherlands: Elsevier Ltd, 2001; pp. 1123–31.

63. Tanaka K. High-pressure structural changes in chalcogenide glasses. Solid State Commun. 1986;58:469–71.

64. Tanaka K. Pressure dependence of the first sharp diffraction peak in chalcogenide and oxide glasses. Phil Mag Lett. 1988;57:183–7.

65. Renninger AL, Averbach BL. Atomic radial distribution functions of As-Se glasses. Phys Rev B. 1973;8:1507–14.

66. Poltavtsev YuG. Structure of semiconductors in non-crystalline states. Usp Fiz Nauk. 1976;120:581–612.

67. Popescu M. Medium range order in chalcogenide glasses. In: Andriesh A, Bertolotti M, editors. Physics and applications of non-crystalline semiconductors in optoelectronics. Dordrecht, Boston, London: Kluwer Academic Publishers, 1997; p. 215–32.

68. Shpotyuk M, Shpotyuk O, Golovchak R, Demchenko P. FSDP-related correlations in γ-irradiated chalcogenide semiconductor glasses: the case of glassy arsenic trisulphide g-As2S3 revised. J Phys Chem Solids. 2013;74:41721–5.

69. Shpotyuk O, Kovalskiy A, Trimble J, Vlcek M, Shpotyuk Y, Kozyukhin S. Intrinsic phase separation in low-temperature quenched arsenic trisulfide glass. J Non-Cryst Solids. 2015;430:16–20.

70. Mori T, Yasuoka H, Saegusa H, Okawa K, Kato M, Arai T, et al. Layer correlation in a-As2(SexS1-x)3 systems. Jpn J Appl Phys. 1983;22:1784–9.

71. Tanaka K. Photoexpansion in As2S3 glass. Phys Rev B. 1998;57:5163–7.

72. Tanaka K. Medium-range structure in chalcogenide glasses. Jpn J Appl Phys. 1998;37:1747–53.

73. Mazets TF, Smorgonskaya EA, Tikhomirov VK. Stable anisotropy in glassy As2S3:In. J Non-Cryst Solids. 1993;164–166:1215–8.

74. Vateva E, Savova E. New medium-range order features in Ge-Sb-S glasses. J Non-Cryst Solids. 1995;192/–193:145–8.

75. Baidakova MV, Faleev NN, Mazets TF, Smorgonskaya EA. Nanoscale medium-range order in semiconducting glassy chalcogenides. J Non-Cryst Solids. 1995;192–193:149–52.

76. Arsova D, Vateva E, Skordeva E, Petkov V. New features of the medium range order in GexAs40-xSe60 glasses. Solid State Commun. 1996;98:595–8.

77. Bonazzi P, Bindi L. A crystallographic review of arsenic sulfides: effects of chemical variations and changes induced by exposure to light. Z Kristallogr. 2008;223:132–47.

78. Kyono A. Molecular conformation and anion configuration variations for As 4S4 and As 4Se4 in an anion-substituted solid solution. Am Mineral. 2009;94:451–60.

79. Aitken BG. GeAs sulfide glasses with unusually low network connectivity. J Non-Cryst Solids. 2004;345–346:1–6.

80. Hrubý A. A study of glass-forming ability and phase diagram of the As-S system. J Non-Cryst Solids. 1978;28:139–42.

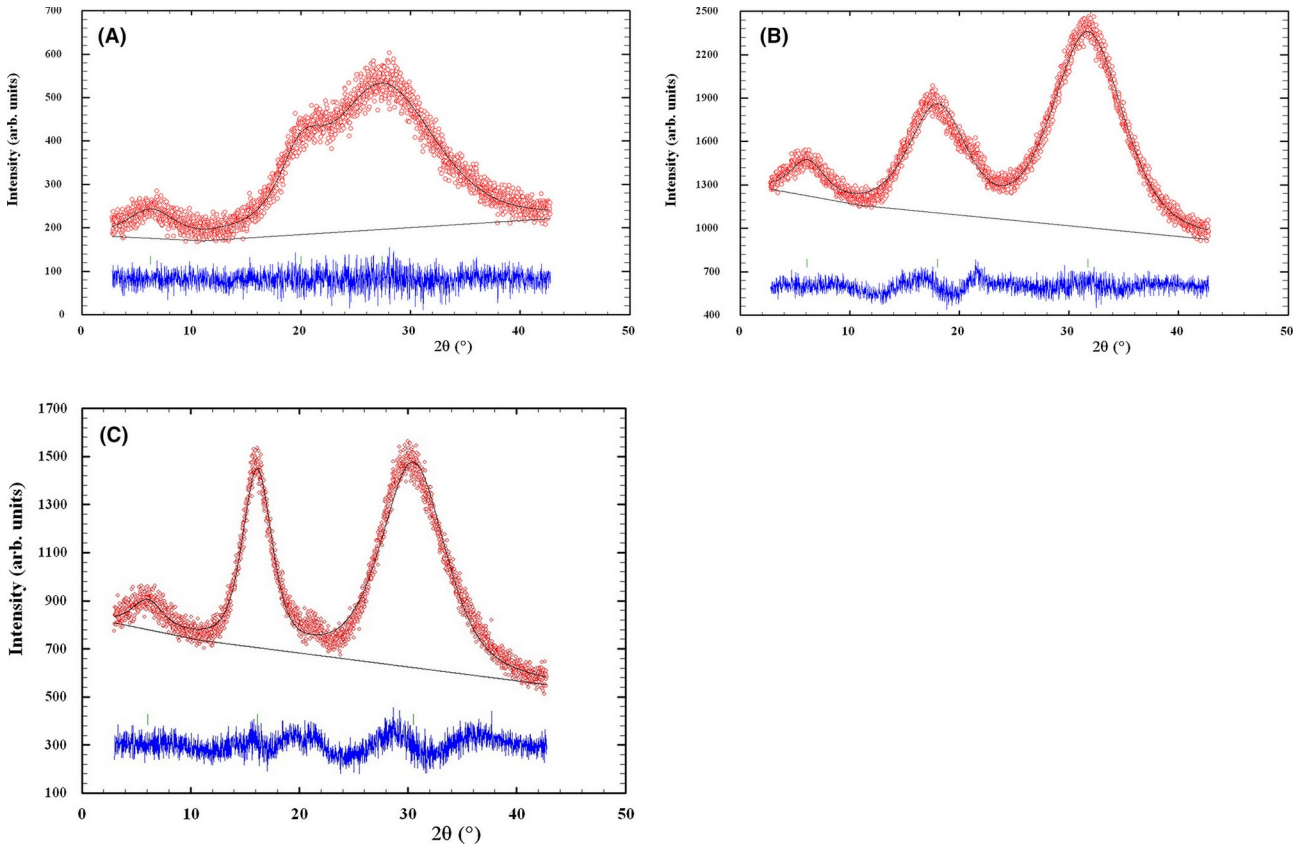

Figure 1. Experimentally observed (red points) and calculated (black solid line) X-ray powder diffraction profiles for unmilled As_5Se_{95} (A), $As_{40}Se_{60}$ (B) and $As_{50}Se_{50}$ (C) showing the first sharp diffraction peak and principal diffraction peak (the difference curve is given at the bottom by blue solid line)

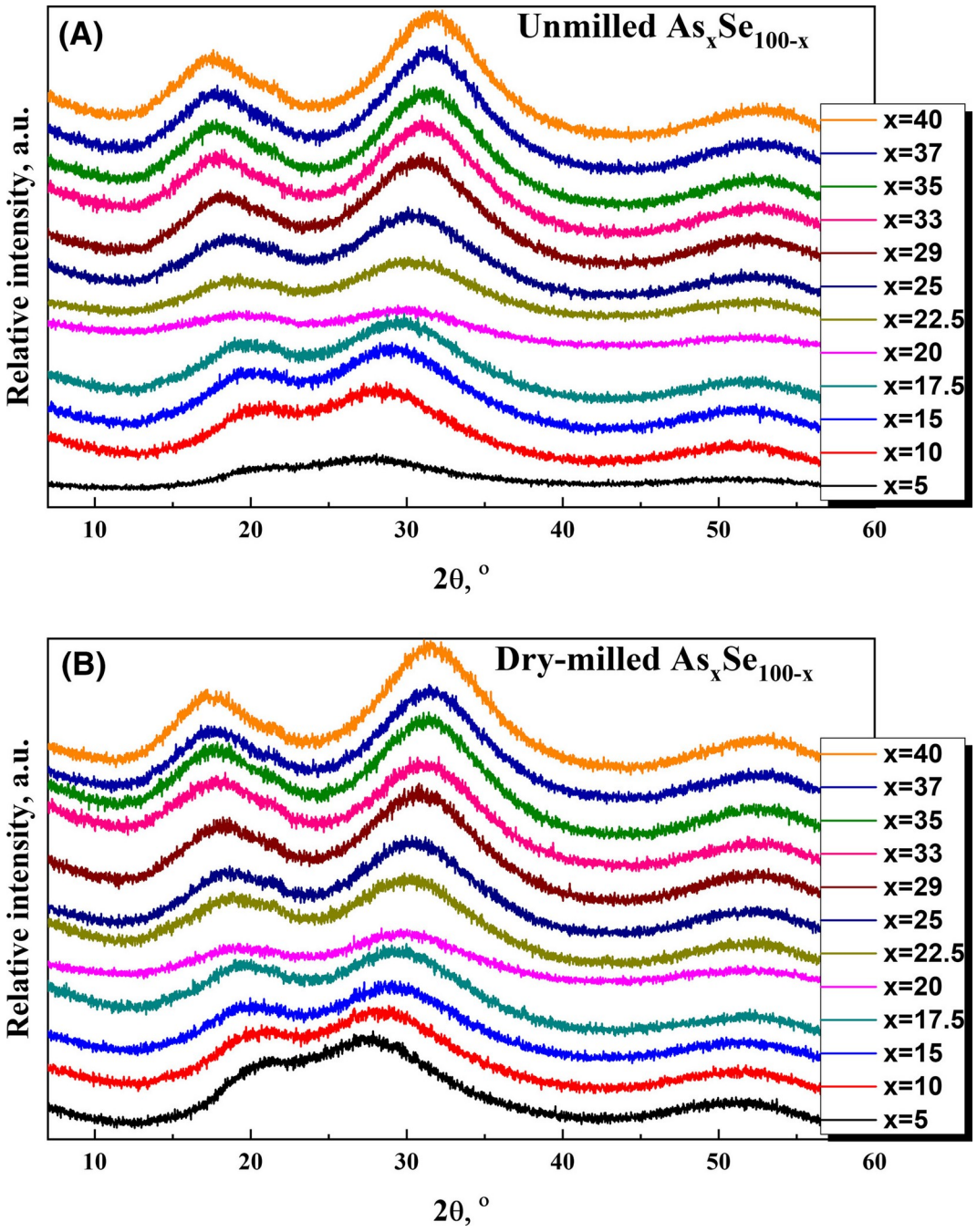

Figure 2. Experimental X-ray powder diffraction profiles for unmilled (A) and dry-milled (B) under-stoichiometric glassy As_xSe_{100-x} ($5 \le x \le 40$) showing diffuse halos (for clarity reason, each curve is offset along *y* axis)

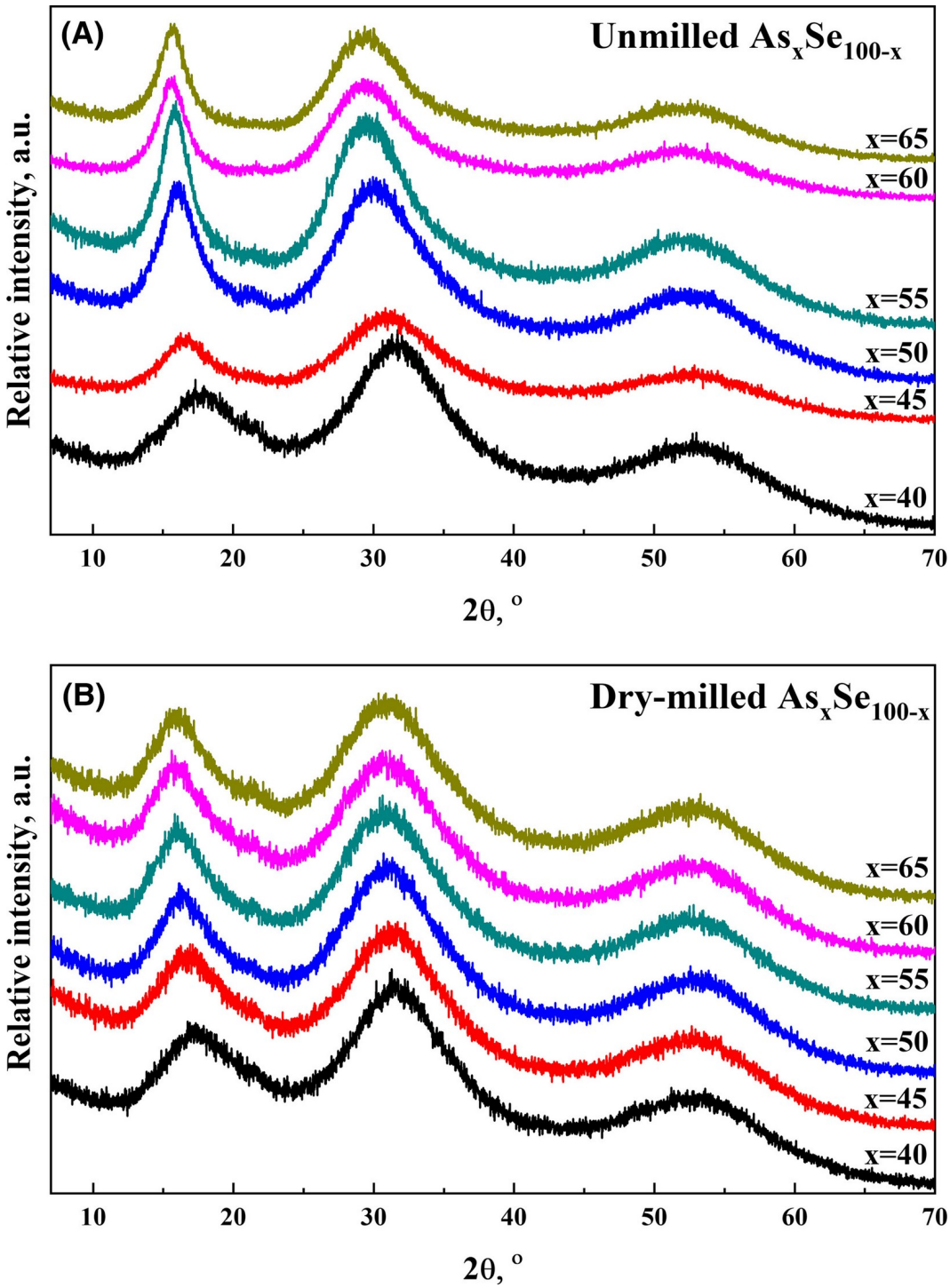

Figure 3. Experimental X-ray powder diffraction profiles for unmilled (A) and dry-milled (B) over-stoichiometric As_xSe_{100-x} ($40 \le x \le 65$) showing diffuse halos (for clarity purposes, each curve is offset along *y* axis)

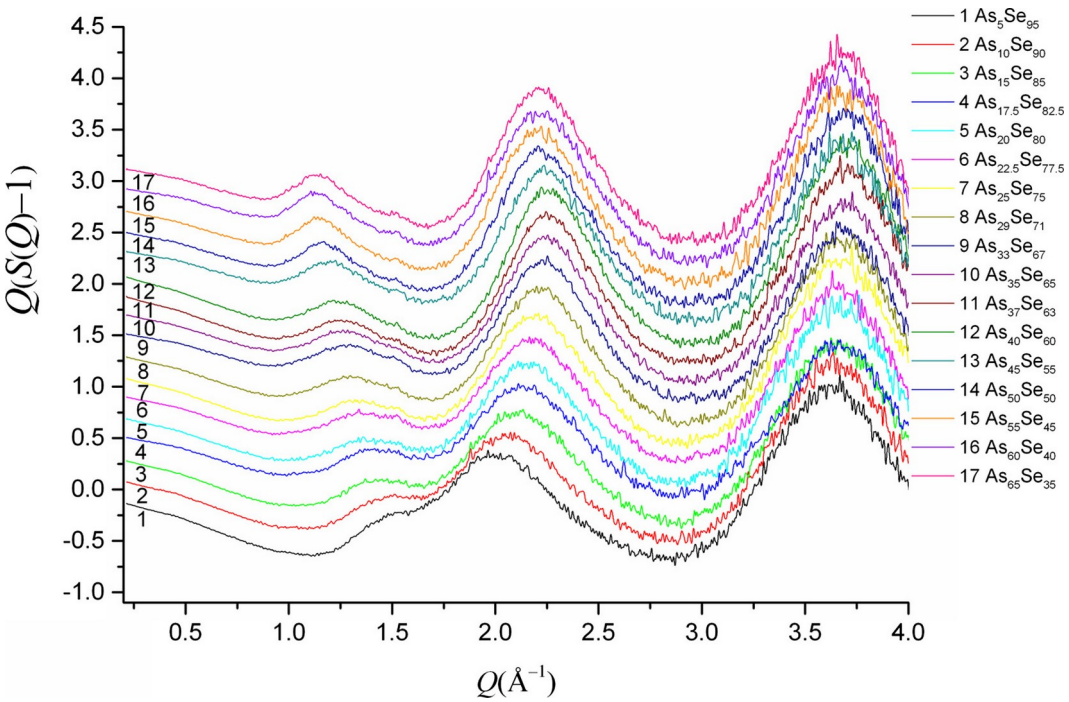

Figure 4. Low-Q part of the calculated reduced X-ray structure factor $F(Q) = Q(S(Q)-1)$ for dry-milled As_xSe_{100-x} (for clarity purposes, each curve is offset along y axis)

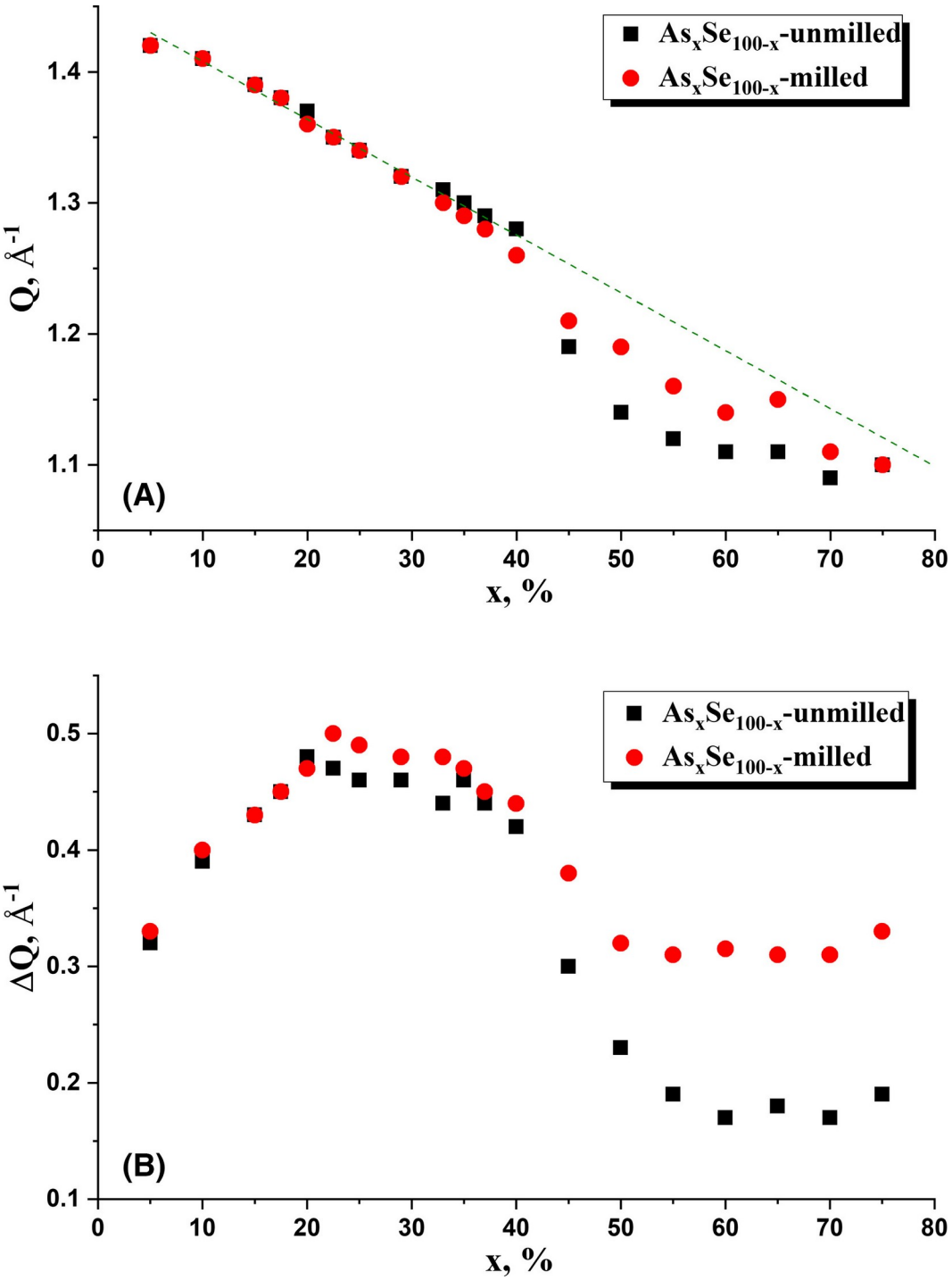

Figure 5. Compositional variations in the first sharp diffraction peak position Q_1 (A) and width ΔQ_1 (B) for As_xSe_{100-x} in unmilled (black squares) and milled (red circles) state

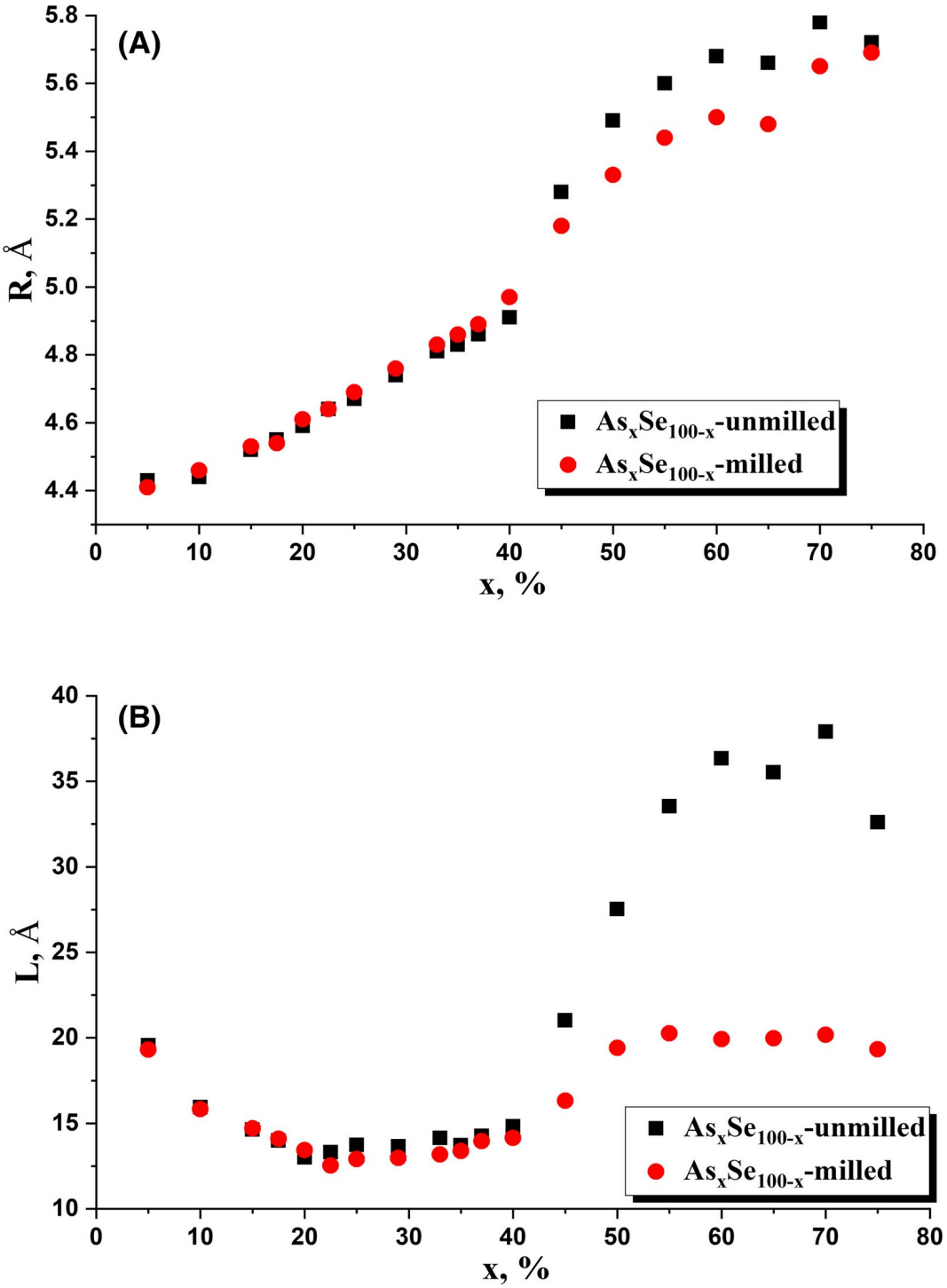

Figure 6. Compositional changes in the first sharp diffraction peak-related X-ray powder diffraction parameters (A, characteristic distance *R*; B, correlation length *L*) for As_xSe_{100-x} in unmilled (black squares) and milled (red circles) state

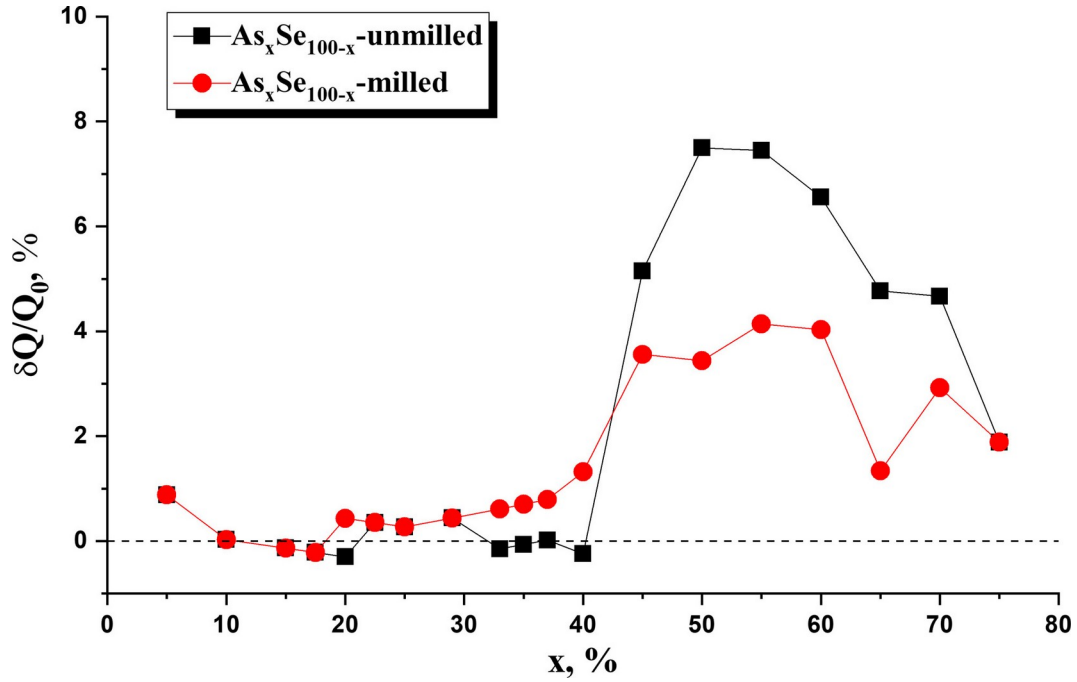

Figure 7. Relative deviation from linear Q(x) dependence for unmilled (black squares) and milled (red circles) As_xSe_{100-x} (linearization is performed for unmilled under-stoichiometric glasses, $5 \le x \le 40$)

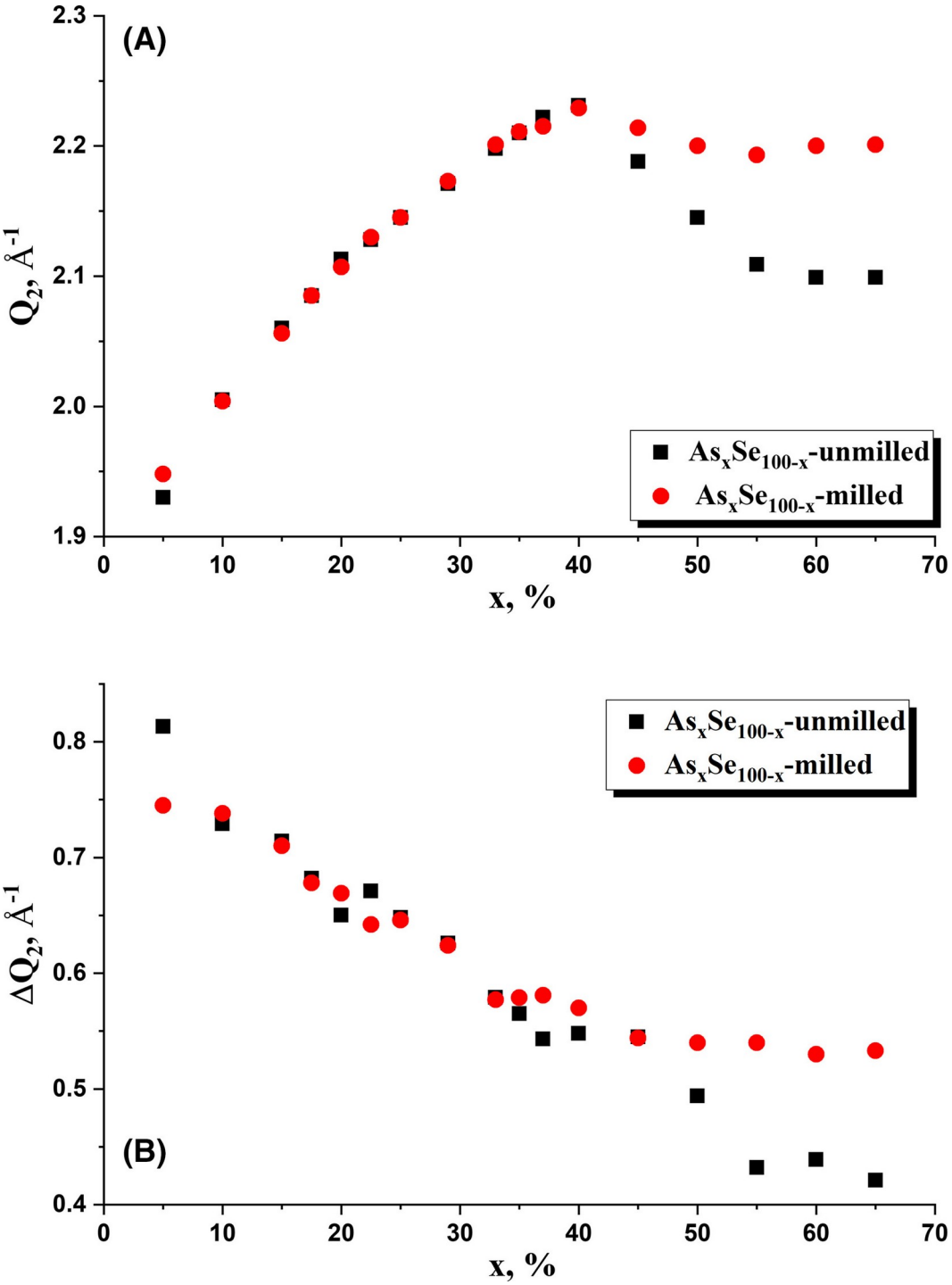

Figure 8. Compositional variations in the PDP position Q_2 (A) and width ΔQ_2 (B) for As_xSe_{100-x} in unmilled (black squares) and milled (red circles) state

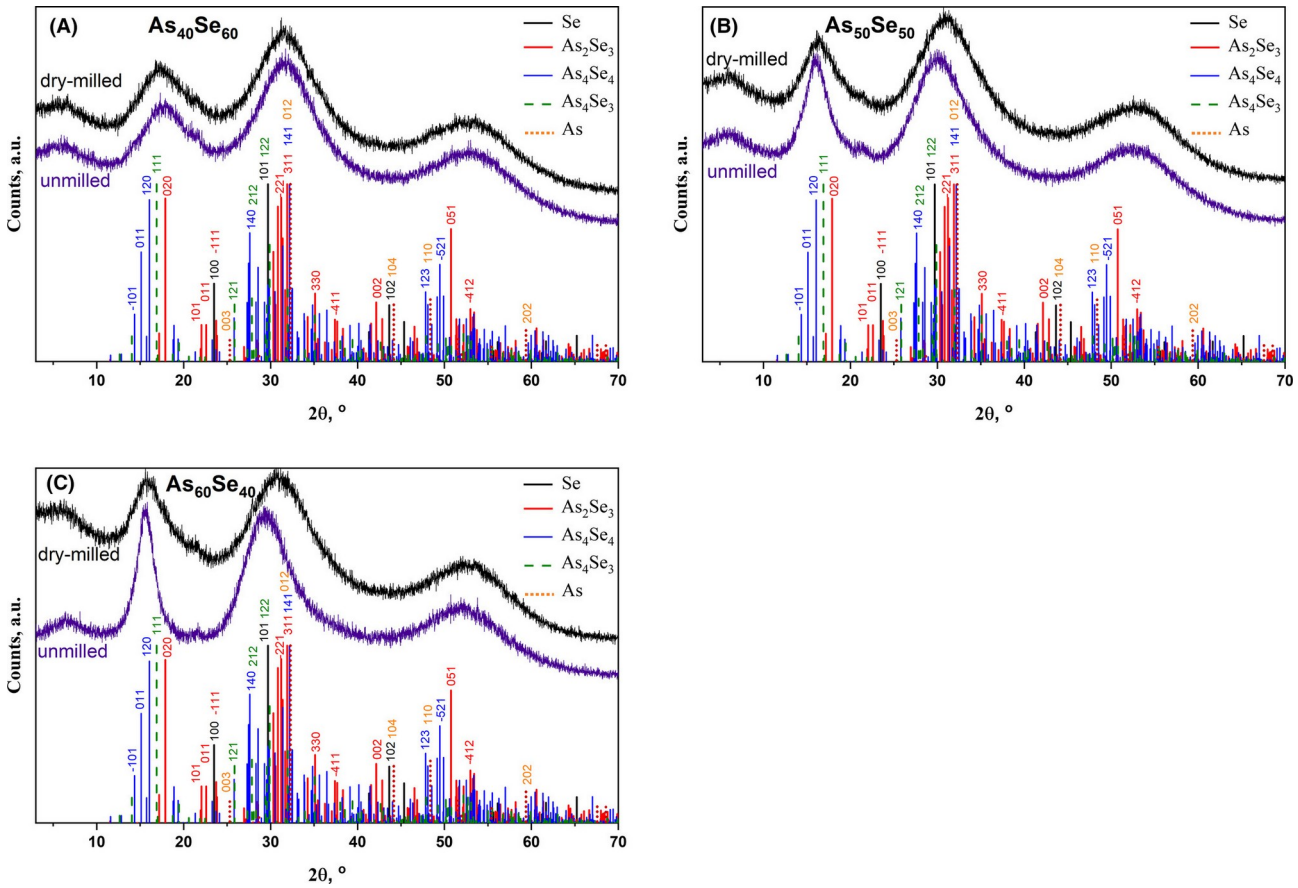

Figure 9. Experimental X-ray powder diffraction patterns of unmilled and dry-milled arsenoselenides $As_{40}S_{60}$ (A), $As_{50}S_{50}$ (B), and $As_{60}S_{40}$ (C) showing diffuse halos at ~15-22 $^{o}2\Theta$ (FSDP), ~28-33 $^{o}2\Theta$ (PDP) and ~50-60 $^{o}2\Theta$ (TDP). Theoretical Bragg-diffraction reflexes for Se, As_2Se_3, As_4Se_4, As_4Se_3 and As are shown for comparison (see text for more details)

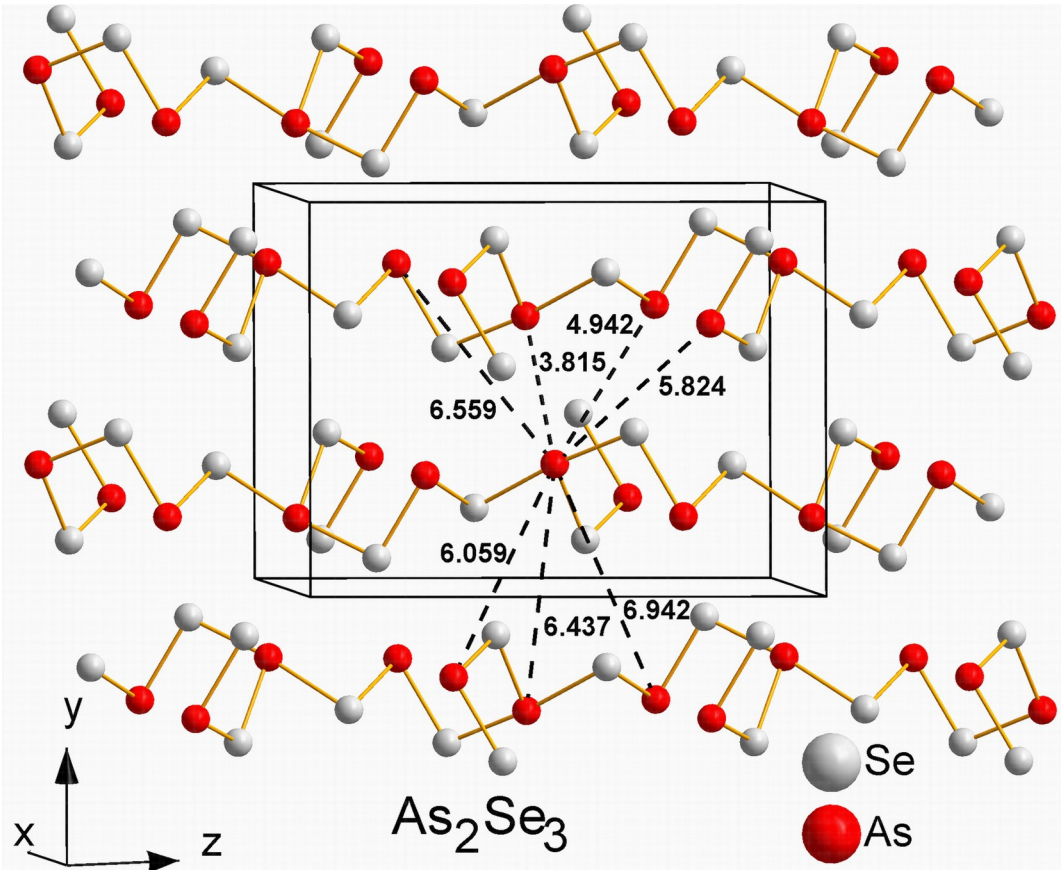

Figure 10. Schematic presentation of neighboring atomic sheets in the layered structure of monoclinic As_2Se_3 separated by (020) *xz*-plane. Selected inter-planar (As)–(As) distances for As atoms belonging to these sheets (in Å) are denoted by dashed lines, As and Se atoms being respectively depicted in red and gray (see text for more details)

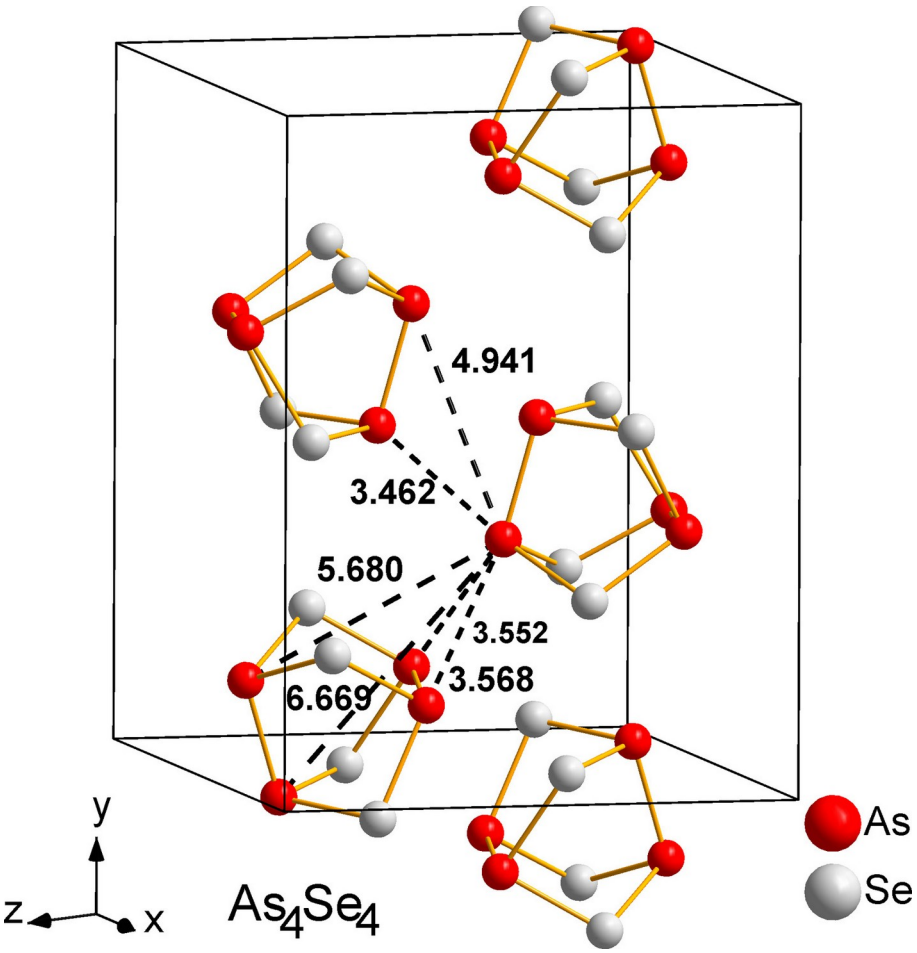

Figure 11. Schematic presentation of neighboring As_4Se_4 molecules in the monoclinic As_4Se_4. For chosen As atom within one As_4Se_4 molecule, selected (As)–(As) distances between As atoms belonging to neighboring molecules (in Å) are denoted by dashed lines, the As and Se atoms being respectively depicted in red and gray (see text for more details)

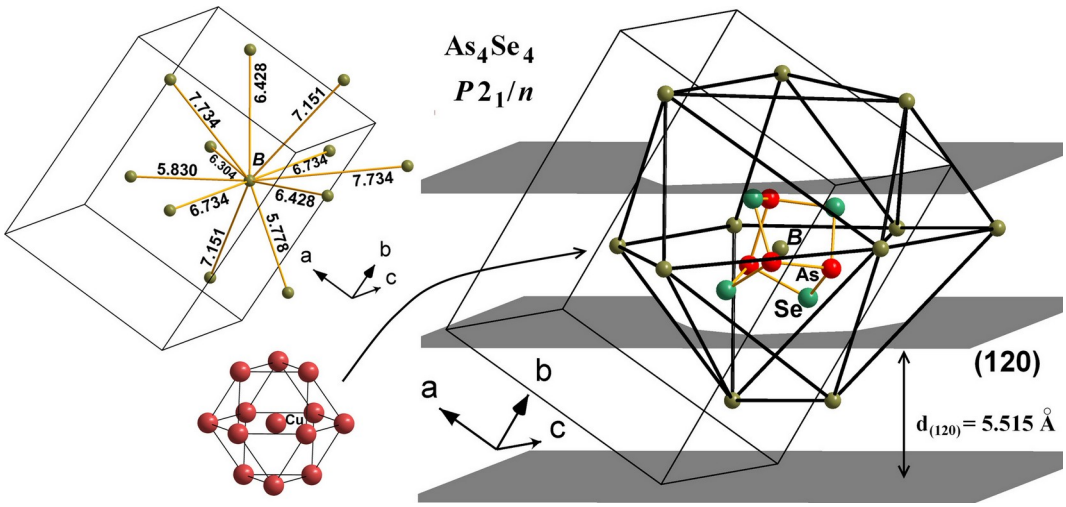

Figure 12. Fragment of As_4Se_4 crystal structure (SG $P2_1/n$, structure type α-As_4S_4 in respect to Kyono[78]), showing all possible inter-molecular centroid-centroid distances B-B in Å (left); packing of As_4Se_4 cage-like molecules (only one molecule is shown for clarity) as the $B[B_{11}]$ polyhedron (right), which can be considered as an incomplete distorted cubooctahedron (face-centered cubic close packing of Cu structure type shown at the bottom left); together with the family of (120) planes corresponding to the *hkl* reflection (120) in the crystal structure of As_4Se_4 (I = 97%)

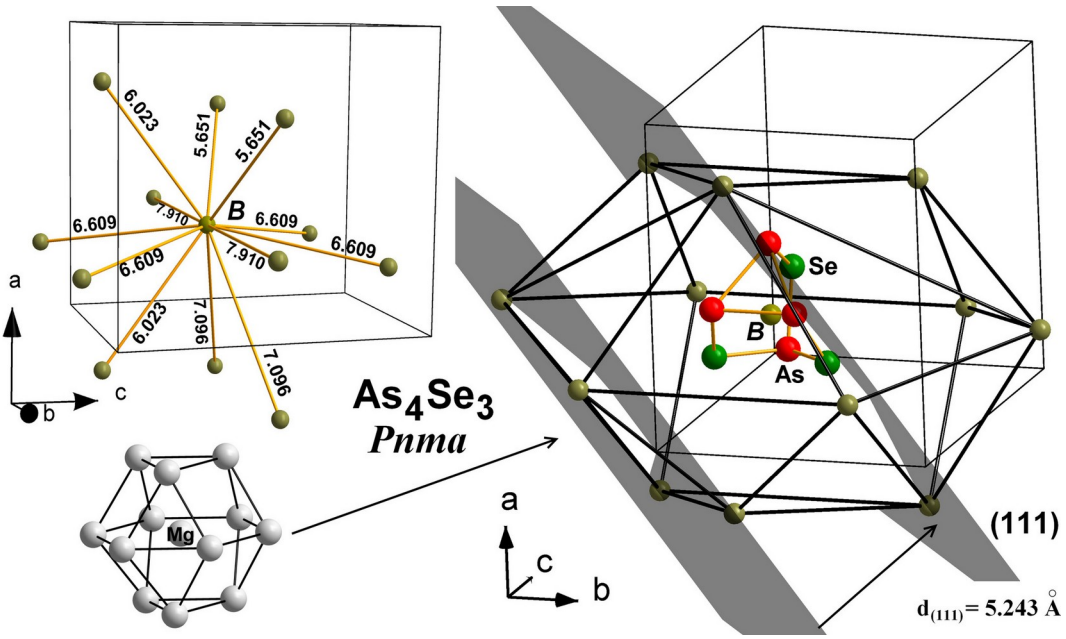

Figure 13. Fragment of As_4Se_3 crystal structure (SG *Pnma*, structure type α-As_4S_3 imorphite high-temperature modification, or β-dimorphite in respect to)[57] showing all possible inter-molecular centroid-centroid distances B-B in Å (left); packing of As_4Se_3 cage-like molecules (only one molecule is shown for clarity) as the $B[B_{12}]$ polyhedron, which can be considered as deformed anticubooctahedron (hexagonal close packing of Mg structure type shown at the bottom left); together with the family of (111) crystallographic planes corresponding to *hkl* reflection (111) in the crystal structure of As_4Se_3 (I = 100%)